Annu. Rev. Earth Planet. Sci. 1992. 20:329–64

THE STRUCTURE OF MID-OCEAN RIDGES

Sean C. Solomon

Department of Earth, Atmospheric, and Planetary Sciences,
Massachusetts Institute of Technology, Cambridge, Massachusetts 02139

Douglas R. Toomey

Department of Geological Sciences, University of Oregon,
Eugene, Oregon 97403

KEY WORDS: crust, mantle, seismic velocity, seismic attenuation, magma chambers

INTRODUCTION

Mid-ocean ridges provide an important window into the processes of mantle convection and magmatism. The formation, cooling, and eventual subduction of oceanic lithosphere dominate both the large-scale dynamics of the upper mantle and the Earth's global heat loss. The melt generated during pressure-release melting of the upwelling mantle beneath mid-ocean ridges contributes most of the annual magmatic flux of the planet. The emplacement and differentiation of that melt at ridge axes reflects a complex interplay of cooling and deformational processes, which are strongly influenced in turn by the rate of plate separation and the detailed geometry in map view of the zone of crustal accretion.

Seismology offers a powerful tool to elucidate the processes of crustal and lithospheric formation and evolution at mid-ocean ridges. Compressional and shear wave speeds are sensitive to bulk composition, fracture and pore volume, and the presence of partial melt. The rates of attenuation of seismic waves are also strong functions of temperature and fracture porosity. Where there is a preferred orientation to anisotropic

0084–6597/92/0515–0329$02.00

minerals, such as shear-induced ordering of mantle olivine crystals, or to prominent structures, such as near-surface fissures or faults, the velocity and attenuation of seismic waves can display an anisotropy diagnostic of the governing process. The ability of a seismic experiment to resolve seismic properties at depth is limited principally by the seismic wavelength and also by experiment design and depth of interest.

While seismology has long been a primary source of information on the vertical structure of oceanic crust and the dependence of crustal and mantle structure on lithosphere age, a number of seismic experiments and related studies in the last 5 years have considerably altered our view of the detailed structure of mid-ocean ridge axes and of the processes by which new oceanic lithosphere forms. Multichannel reflection seismology is becoming increasingly used to map prominent structural boundaries, such as the tops of magma bodies in the axial crust and the top of the crust-mantle transition. Body wave tomography is being applied to large data sets from active seismic experiments to produce high-resolution images of seismic velocities and attenuation in two and three dimensions. Surface wave phase velocities and arrival times of direct and surface-reflected body waves at teleseismic distances, both in regional studies and as parts of global upper mantle tomographic inversions, are being employed to investigate the ocean ridge mantle in increasingly fine detail.

This paper reviews these recent results on the structure of mid-ocean ridges. After a brief introduction to the now-classical models of oceanic crustal structure and of ocean crustal formation, we turn to the new view of ridge-axis crustal structure from high-resolution seismology, particularly to the variation of that structure with spreading rate and along-axis at a given spreading rate. The details of these structural variations now constitute strong constraints on the nature of axial magma chambers and the relation of magmatism to morphological segmentation of the rise axis. We then review recent results on upper mantle structure beneath ridges, including variations with seafloor age, indications from anisotropy for directions of mantle flow, and long-wavelength along-axis variations in structure and their implications for lateral heterogeneity in mantle temperature and composition. Finally, we close with a summary of several outstanding issues in our understanding of mid-ocean ridge processes and offer suggestions for future seismic experiments to address these issues.

STRUCTURE OF MATURE OCEANIC CRUST AND UPPER MANTLE

It has been known for several decades that mature oceanic crust far from the axes of crustal accretion is vertically layered and is typically about 6–

7 km thick, largely independent of spreading rate (Raitt 1963, Reid & Jackson 1981). With improvements in seismic instrumentation, experiment design, and analysis techniques, the early view of the oceanic crust as a small number of homogeneous layers (Raitt 1963) was replaced by structural models involving smooth variations in velocity with depth and sharply depth-dependent vertical gradients in velocity (Spudich & Orcutt 1980). A typical distribution of *P*-wave velocity with depth in oceanic crust is shown in the upper part of Figure 1.

The interpretation of velocity structure in terms of lithology has been based on analogy with structures in ophiolite complexes and by comparison of velocities measured in laboratory samples from dredged rocks, oceanic drill cores, and ophiolites with the velocities measured in refraction experiments (Fox et al 1973, Christensen & Salisbury 1975, Spudich & Orcutt 1980, Casey et al 1981, Bratt & Purdy 1984). One such interpretation is given in Figure 1. The upper oceanic crust, or layer 2 of Raitt (1963), is thought to grade downward from volcanic flows and pillow basalts into a complex of sheeted diabase dikes. This upper portion of the classical ophiolite lithostratigraphy has been observed in a 1-km-deep drill hole in oceanic crust (Anderson et al 1982). The mid to lower crust, or layer 3 of Raitt (1963), has properties appropriate to the massive to cumulate gabbro layer seen in ophiolite complexes, and the uppermost oceanic mantle has a seismic velocity appropriate for depleted peridotite. On the basis of seismic refraction data, particularly amplitude-range information, and field studies in ophiolites, the boundaries between the principal layers likely display both considerable vertical complexity and significant lateral variability (Casey et al 1981, Bratt & Purdy 1984).

Seismic refraction studies in the oceans have shown that the uppermost oceanic mantle is azimuthally anisotropic, with the fast direction for *P* waves generally coincident with the spreading direction at the time of formation of the overlying crust (Hess 1964, Raitt et al 1969, Shimamura 1984, Shearer & Orcutt 1985). This pattern of anisotropy has also been observed for Rayleigh waves (Forsyth 1975, Nishimura & Forsyth 1988) and lithospheric guided waves (Butler 1985). The anisotropy is believed to result from the preferential alignment of the high-velocity *a*-axis of mantle olivine crystals during the shear strain accompanying the formation and growth of oceanic lithosphere (Hess 1964, Francis 1969). The range of wave types, periods, and distance intervals over which azimuthal anisotropy has been documented suggests that this pattern of anisotropy extends throughout most, if not all, of the mantle portion of oceanic lithosphere.

The vertical structure of oceanic crust is the result of injection, cooling, eruption, and solidification of basaltic magma generated by adiabatic decompression of the column of upwelling mantle beneath the mid-ocean

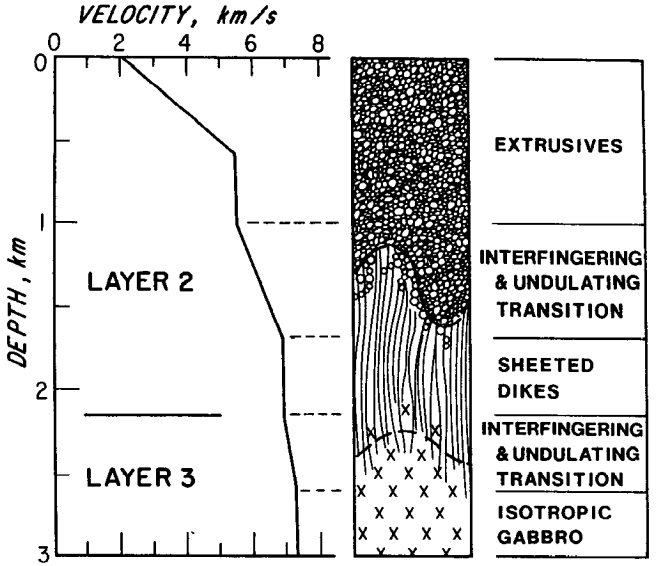

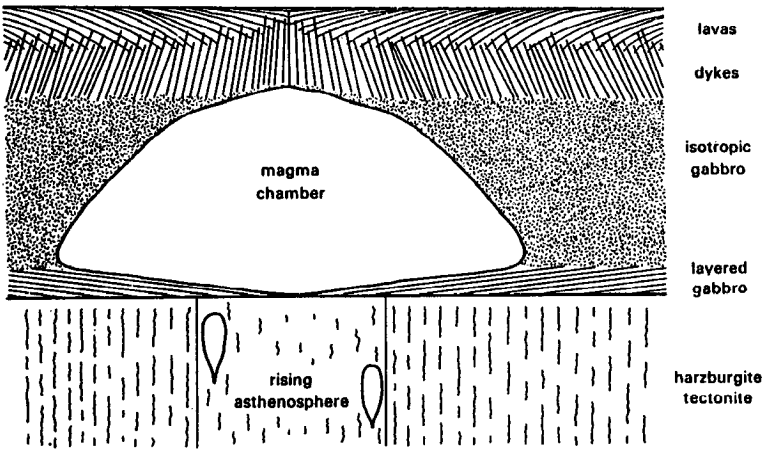

Figure 1 (*Top*) Generalized *P*-wave velocity structure of the upper oceanic crust and a geological interpretation (after Bratt & Purdy 1984) based on deep-sea drilling results and studies of ophiolite complexes. (*Bottom*) A possible schematic structure of a large ridge-axis magma chamber and its relation to oceanic crustal layering (from Cann 1974).

ridge axis. Models for crustal formation developed 10–20 years ago were influenced strongly by field geological observations in ophiolite complexes. They featured large magma chambers (Figure 1) which at least episodically filled the mid to lower oceanic crust and had cross-axis dimensions of a few to several tens of kilometers, depending on ridge spreading rate (Cann 1974, Kidd 1977, Casey & Karson 1981). According to these models, eruptions from these magma chambers form the effusive upper crustal layer and the underlying system of vertical dikes, and slow cooling and solidification of the chamber along its walls and at its base form the massive gabbro layer of the middle oceanic crust and the underlying mafic and ultramafic cumulate layers, respectively, with the downward transition to principally ultramafic material marking the top of the seismologically defined mantle. Such magma chambers should have strong signatures in the seismic structure of ridge-axis regions, and the search for and delineation of axial magma chambers (AMCs) has been the focus of a number of recent seismic experiments. The region of upwelling, melt generation, and vertical magma transport in the ridge-axis upper mantle poses a greater challenge to geophysical observation and has to date been comparatively unstudied.

RECENT RESULTS ON RIDGE-AXIS CRUSTAL STRUCTURE

In the last 10 years it has been increasingly recognized that the mid-ocean ridge is not a simple two-dimensional structure but rather varies systematically along its axis. The application of high-resolution bathymetric swath mapping and deep-towed and submersible observations of fine-scale volcanic, tectonic, and hydrothermal features has revealed that the ridge axis may be divided into distinct segments some 10–100 km in length bounded by structural features or morphological boundaries such as an offset in the location or trend in the axis of most recent crustal accretion. Several scenarios linking this segmentation to the production and transport of melt in the upper mantle have been advanced. According to these scenarios, ascending melt is focused, either by enhanced rates of melt production (Francheteau & Ballard 1983) or enhanced rates of upwelling (Whitehead et al 1984, Crane 1985, Schouten et al 1985), into magmatic centers spaced 10–100 km along the axis. Each magmatic center supplies the majority of heat and melt to the crust beneath a single ridge segment. Within each segment, the characteristics of faulting, hydrothermal circulation, and magmatic accretion vary systematically with distance from the magmatic center (Francheteau & Ballard 1983, Schouten et al 1985).

Recent work on the seismic structure of the crust along the axis of active spreading centers has illuminated and sharpened the concept of segmentation and its relationship to axial magmatism. Both the forms of segmentation and the seismic structure of the crust differ between fast-spreading (full divergence rates of about 70 mm/yr and greater) and slow-spreading (divergence rates less than about 70 mm/yr) ridges. We therefore divide the discussion to follow by spreading rate. Typical examples of the two classes of ridge systems are, respectively, the East Pacific Rise and the Mid-Atlantic Ridge.

Fast-Spreading Rises

Thermal models for mid-ocean ridges predict that shallow crustal temperatures are generally higher along faster spreading rises and that axial magma chambers may be steady-state features (Sleep 1975). The East Pacific Rise has thus been the focus of a number of different types of seismic experiments designed to investigate the cross-sectional shape of axial magma chambers, the along-axis variability in structure, and the relationship of structural variability to seafloor bathymetry, morphology, and tectonics and to the chemistry of seafloor basalts. Most of these studies have concentrated on a limited section of the northern East Pacific Rise between about 9° and 13°N (Figure 2). Important recent experiments include the multichannel seismic reflection imaging of the cross-axis and along-axis continuity of the top of the axial magma chamber (Detrick et al 1987, Mutter et al 1988), the modeling of *P*-wave travel times and amplitudes in two sets of expanding spread profiles (ESPs) shot along and parallel to the rise axis (Harding et al 1989, Vera et al 1990), and the two-dimensional (Burnett et al 1989, Caress et al 1992, Wilcock et al 1991) and three-dimensional (Toomey et al 1990) tomographic imaging of seismic velocity and attenuation in the rise axis region.

SHALLOW CRUST The uppermost kilometer of young oceanic crust, comprising the extrusive flows and pillow basalts and at least a portion of the sheeted dike complex, is the result of volcanic construction. This depth interval undergoes a systematic and geologically rapid evolution in seismic structure near the rise axis. The top 200–400 m of the igneous crust of the rise axis region is characterized by low seismic velocities ($V_p \sim 2$–3 km/s), low Q, and a high bulk porosity of 10–20% (Herron 1982, Harding et al 1989, Vera et al 1990). Within a narrow zone centered approximately along the rise axis, however, the velocity and Q averaged over the upper 1 km are both high ($V_P \sim 4$–5 km/s, $Q \sim 40$–50) relative to the velocity and attenuation averaged over this depth interval only 1–2 km from the neovolcanic zone (McClain et al 1985, Burnett et al 1989, Toomey et al 1990,

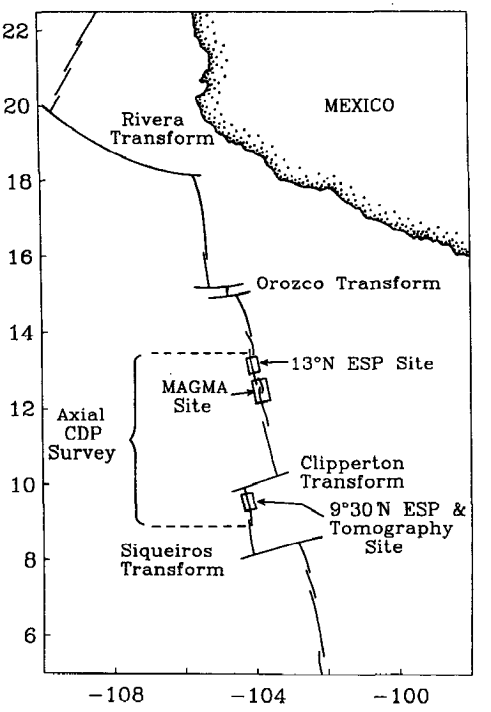

Figure 2 Sites of important seismic experiments along the axis of the northern East Pacific Rise (from Caress et al 1991). Two-dimensional (Burnett et al 1989, Caress et al 1992) and three-dimensional (Toomey et al 1990) tomography experiments were conducted at the MAGMA site (McClain et al 1985) and at 9°30′N, respectively.

Wilcock et al 1991); see Figure 3. Where along-axis coverage is available, the axial high-velocity (Toomey et al 1990), high-Q (Wilcock et al 1991), shallow-crustal anomaly is a persistent feature of the rise crest. The preferred interpretation is that the sheeted dike complex at zero age lies at shallower depths than beneath normal seafloor (Cann 1974, Kidd 1977, Toomey et al 1990). The rapid change within 1–2 km of the axis to lesser upper-crustal seismic velocities and Q is, by this view, the result of repeated eruptions of porous basalts which progressively thicken the extrusive carapace. Resolving the spatial and temporal nature of these axial variations in seismic characteristics and relating the seismic properties to bulk porosity and permeability should provide important constraints on models for hydrothermal circulation through the shallow crust of the rise axis region.

In addition to volcanic eruptions, both tectonic and hydrothermal pro-

cesses may induce age-dependent variations in porosity or composition of the upper oceanic crust that are detectable by seismic methods (McClain et al 1985, Burnett et al 1989, Wilcock et al 1991). In support of this view are several observations indicating that shallow crustal seismic velocities continue to evolve to distances well beyond a few kilometers from the axis (Houtz & Ewing 1976, Herron 1982, Purdy 1982). Several hypotheses have been put forward to explain aging of the shallow crust, including increases in bulk porosity due to the formation of cracks and, perhaps at least partly on a longer time scale, metamorphic alteration and mineral precipitation during hydrothermal circulation.

AMC REFLECTOR Despite the predictions from thermal models and observations in ophiolites for a melt-filled axial magma chamber as much as 10 km wide and several kilometers in thickness (Cann 1974, Sleep 1975, Bryan & Moore 1977, Casey & Karson 1981, Pallister & Hopson 1981), the various seismic experiments designed to test these predictions along the northern East Pacific Rise have to date imaged only a comparatively narrow, axially discontinuous melt lens (Hale et al 1982, Herron et al 1978, Detrick et al 1987, Kent et al 1990). The best evidence for the existence of even a small axial magma body comes from the high-amplitude, subhorizontal upper crustal reflector seen on multichannel seismic profiles across the rise axis; the amplitude of the reflector versus range and its phase reversal relative to the seafloor reflection at some locations indicate that it marks the roof of a partially to fully molten layer. An example of a multichannel seismic reflection image of the top of the East Pacific Rise AMC in cross section is shown in Figure 4. Between about 9° and 13°N, the depth of the axial reflector ranges between 1.6 and 2.4 km beneath the seafloor (Detrick et al 1987), with increasing depth to the reflector correlating with increased bathymetric depth. Carefully migrated multichannel seismic data constrain the maximum width of the AMC reflector to be less than 3–4 km across the axis (Hale et al 1982, Herron et al 1978, Detrick et al 1987); more recent modeling of diffraction hyperbolas generated by the reflector's edge indicate an upper limit to the cross-axis width of as little as 800–1200 m (Kent et al 1990). Under the assumption that the base of the melt-filled sill marks a sharp contrast in seismic impedance, the reflected waveforms along the axis are consistent with a melt lens only 10–50 m thick (Kent et al 1990); however, if the bottom of the lens changes gradually from melt to a crystalline mush over a depth interval of several hundred meters or more, then the nature of this transition is poorly constrained by reflected wave amplitudes.

Reflected wave amplitude and phase data also constrain the physical characteristics of the AMC, including the nature of the solid-melt interface

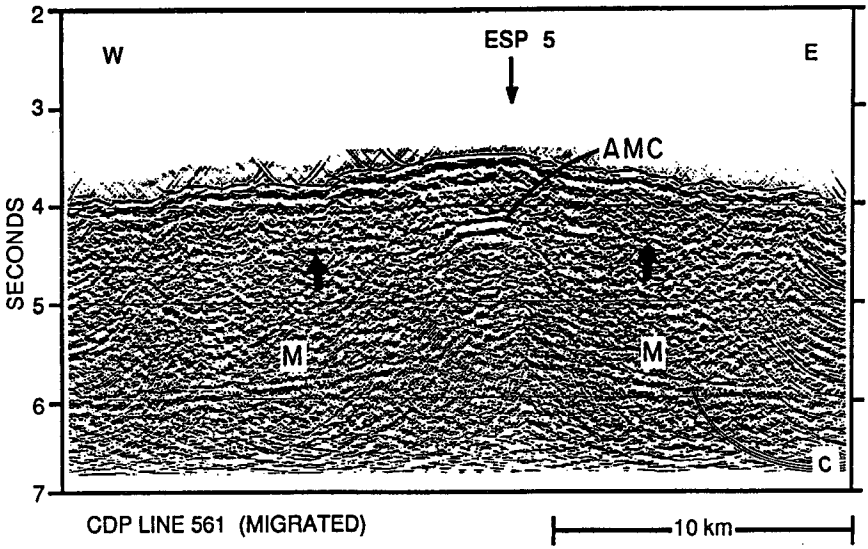

Figure 4 Multichannel seismic reflection profile across the East Pacific Rise near 9°30′N (from Detrick et al 1987). The high-amplitude, sub-horizontal reflector present beneath the rise axis is interpreted as the top of the axial magma chamber (AMC). Reflections from the Moho (*M*) can be traced to within 2–3 km of the rise axis. The arrows indicate a weak reflector interpreted as the top of a frozen magma chamber. This profile crosses the rise axis very near the cross-sections shown in Figure 3.

at the reflector boundary and the material properties of melt within the lens. At normal incidence the *P*-wave reflection coefficient is controlled largely by the contrast in compressional velocity across the reflector. At nonzero offset or range, however, the reflection coefficient is sensitive to discontinuities in the shear modulus, a circumstance that allows inferences regarding the state of the magma lens. At 9°30′N, where a bright AMC reflector is observed on normal-incidence reflection profiles, the nonzero-offset data indicate that the melt is fully molten, i.e. the shear modulus is effectively zero (Vera et al 1990). In contrast, near 13°N, the normal-incidence AMC reflector is considerably weaker and the inferred shear velocities are most consistent with a partially molten lens (Harding et al 1989). Along the northern East Pacific Rise the reflection data are consistent with a vertical-incidence reflection coefficient that varies between 0.2 and 0.4 (Harding et al 1989, Vera et al 1990), with smaller and larger values being consistent with a partially and fully molten lens, respectively. These differences in the AMC reflector are likely expressions of a temporal as well as a spatial variability to crustal magmatism.

Tomographic images of the volume immediately encompassing the AMC reflector (Figure 3) show pronounced anomalies in velocity and attenuation (Toomey et al 1990, Wilcock et al 1991). *P*-wave velocities averaged over a volume of 1 km^3 are anomalously low by as much as 1.5 km/s, and values of apparent Q are less than 20. The cross-axis distributions of V_P and Q are somewhat incongruent, in that velocity anomalies occupy a larger volume than the most pronounced attenuation anomalies. Such differences may result from a dissimilar response of compressional velocity and Q to temperature and melt fraction, as well as from a contribution to apparent attenuation from scattering of energy by the melt lens.

AXIAL LOW-VELOCITY VOLUME The upper crustal melt lens beneath the East Pacific Rise axis caps a significantly larger volume of anomalously low compressional wave velocity (McClain et al 1985, Burnett et al 1989, Harding et al 1989, Vera et al 1990, Toomey et al 1990, Caress et al 1992). The maximum cross-axis width of this low-velocity volume (LVV) is about 5–7 km, well exceeding that of the melt lens; the depth to the top of the LVV gradually increases with distance from the axis (Figure 3). The average compressional velocity within the LVV is about 5.5 km/s. The LVV, however, is not a homogeneous structure. Rise-parallel ESP data (Harding et al 1989, Vera et al 1990) and tomographic imaging (Toomey et al 1990) indicate that velocity within the LVV increases with axial distance. Tomographic data indicate that vertical velocity gradients are positive at mid- to lower-crustal depths (Toomey et al 1990). The structure of the base of the LVV is not known, but analysis of along-axis ESP data (Harding et al 1989, Vera et al 1990) suggests that the lower boundary may be within the lower crust. On the basis of laboratory measurements of compressional wave velocity in basaltic rock and melt (Murase & McBirney 1973), the seismic properties of the axial LVV are consistent with elevated temperatures but do not require the presence of significant partial melt.

Less is known about the *P*-wave attenuation and shear wave velocity structure of the mid to lower crust of the East Pacific Rise axis, but existing information contrasts somewhat with the general characteristics of the *P*-wave LVV. The axial attenuation anomaly appears more subdued in the lower crust than in the volume immediately surrounding the AMC reflector (Wilcock et al 1991), but this may at least partly reflect variations in scattering. The single measurement of shear wave structure at the East Pacific Rise axis (Bratt & Solomon 1984), at the site of a bright AMC reflector on multichannel seismic reflection images, suggests that a large volume of anomalously low *S*-wave velocity is not present at mid-crustal depths.

MOHO AND UPPER MANTLE At least parts of the crustal LVV are underlain by a distinct crust-mantle boundary, or Moho. Cross-axis multichannel reflection data frequently show a Moho signal beneath the rise-axis region (Detrick et al 1987), but this signal is generally absent in the immediate area of the AMC reflector (Figure 4), either because of the absence of a reflecting Moho or because of the attenuation of energy beneath the AMC reflector. Further, observations of Moho arrivals (*PmP*) are reported for ESP lines along and near the rise axis (Harding et al 1989, Vera et al 1990). Amplitude modeling suggests that the Moho is not a single discontinuity but is rather a gradual transition zone about 1 km thick (Vera et al 1990). A summary of the cross-axis structure of the East Pacific Rise near 9°30′N (Figure 5) includes a 1-km-wide AMC reflector, a 6–7-km-wide LVV, and a normal crustal thickness (~6 km) and distinct Moho attained within 1–2 km of the rise axis.

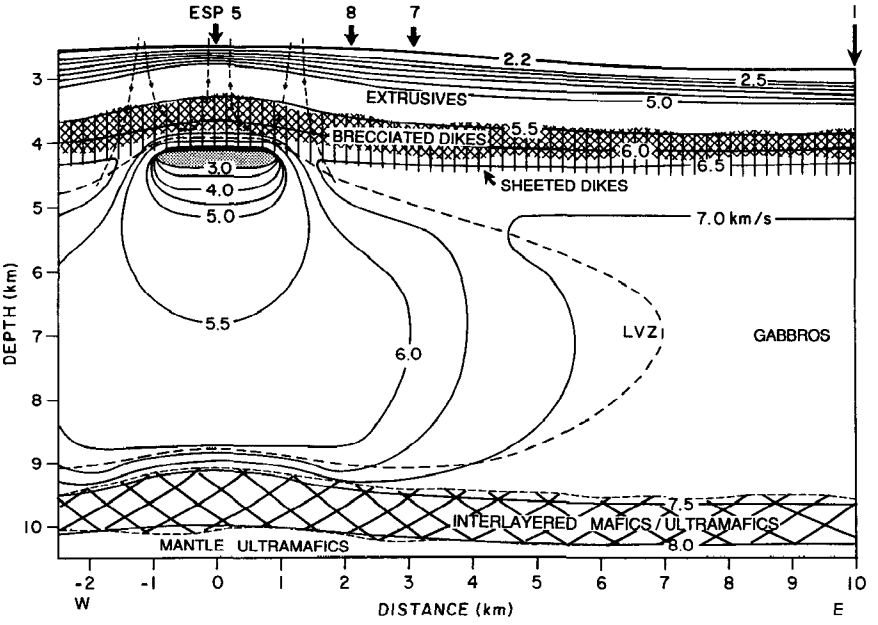

Figure 5 Interpretative summary of the *P*-wave velocity structure (contours in km/s) across the East Pacific Rise axis near 9°30′N (from Vera et al 1990). The summary incorporates the results of cross-axis multichannel seismic reflection profiles (Figure 4) and along-axis ESP data (locations indicated by numbered arrows). The shaded area beneath the axis indicates the inferred magma lens. Conjectural patterns of hydrothermal circulation are indicated by dashed lines and arrows.

There are indications from *P*-wave delay time (Toomey et al 1990) and attenuation (Wilcock et al 1991) tomography for anomalous structure near the Moho beneath the rise axis at 9°30′N. The depth and extent of this anomaly are poorly defined at present. It is apparent, however, that the mid- to lower-crustal LVV is underlain by a second velocity inversion located near the Moho, perhaps within the uppermost mantle. Similarly, the upper crustal low-Q zone overlies a zone of relatively higher Q in the lower crust but apparently lower Q at near-Moho depths.

ALONG-AXIS VARIATIONS The East Pacific Rise is known to vary along its axis in its overall depth, its cross-sectional shape, and its distribution of tectonic and hydrothermal features (Macdonald et al 1988, Haymon et al 1991). Piecewise linear segments of rise are offset by transform faults and overlapping spreading centers of a variety of dimensions (Macdonald et al 1988) or are delimited by modest changes in the trend of the morphological axis without a distinct offset (Langmuir et al 1986). Such tectonic and morphologic segmentation of the rise is also accompanied by segmentation of seismic structure (Figure 6). The AMC reflector terminates near fracture zones (Detrick et al 1987) and is discontinuous at major overlapping spreading centers (Mutter et al 1988). Near morphologically-defined deviations from axial linearity (devals), which can be

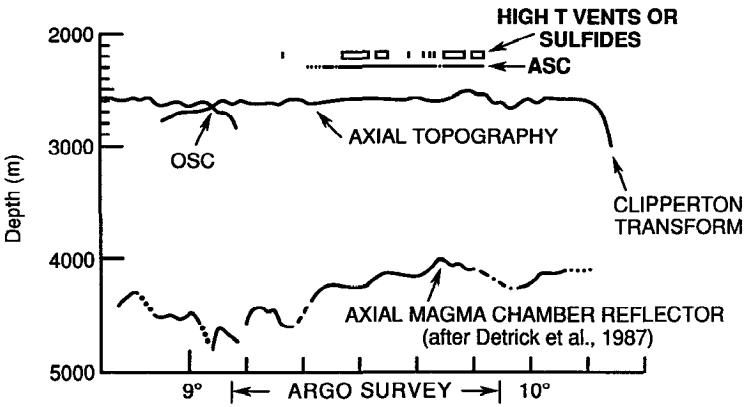

Figure 6 Summary (Haymon et al 1991) of variations in bathymetry, depth to the AMC reflector (from Detrick et al 1987), development of an axial summit caldera (ASC) or graben, and locations of high-temperature hydrothermal vents and sulfide deposits along the East Pacific Rise axis between about 9° and 10°N. The along-axis extent of the survey by the deep-towed ARGO imaging system (the results of which were used to locate the ASC, vent fields, and sulphide deposits) is shown by arrows. The position of a prominent overlapping spreading center (OSC) is also indicated.

accompanied by changes in the average major element chemistry of seafloor basalts (Langmuir et al 1986), the AMC reflector can be discontinuous, abruptly dipping, or continuous (Detrick et al 1987).

Overall the AMC reflector is present along slightly more than 60% of the rise axis between 9° and 13°N (Detrick et al 1987). The reflector appears to be discontinuous for the 90-km section of rise between the Clipperton transform and an overlapping spreading center at 9°03′N—a section that includes several morphologic discontinuities. Detrick et al (1987) proposed that a continuous magma chamber exists along this section of the East Pacific Rise and that this tectonically bounded segment constitutes a spreading center cell that is centrally fed by mantle-derived melt. In contrast, the AMC reflector is absent over the 70-km section of rise to the immediate north of the Clipperton transform (Detrick et al 1987). Other postulated indicators of crustal magma, such as axial depth, axial summit morphology, and width of the axial summit graben (Macdonald et al 1988), also point to a greater melt volume to the south of the Clipperton than to the north. Such variations have not been fully explained but suggest that melt delivery from the mantle is time dependent on scales of 10–100 km.

A different view of axial thermal and magmatic segmentation is emerging from the results of seismic tomography experiments (Toomey et al 1990), which are sensitive to volumetric variations in velocity rather than the sharp contrasts in seismic impedance that are the targets of seismic reflection profiles. The area of the tomographic experiment at 9°30′N was a 15-km-long portion of the rise between the Clipperton and the 9°03′N overlapping spreading center and included two morphologically-defined devals that also coincide with offsets of the axial summit graben (Haymon et al 1991). Three-dimensional images show an axially segmented LVV with the distal ends of the seismic anomaly coinciding with the positions of discontinuities in the trend of the rise axis and the summit graben. These results imply thermal segmentation of the rise axis at the 10-km scale and suggest that this scale of segmentation is imposed by the dynamics of melt generation and transport rather than by tectonic structures in the lithosphere. In this view, the 90-km-long tectonic segment between the Clipperton transform and the 9°03′N overlapping spreading center would encompass several volcanically-defined segments, each centered on a distinct site of injection of melt to upper crustal levels.

Slow-Spreading Ridges

At slower spreading rates the axial crust is significantly cooler than along faster spreading rises (Sleep 1975). As a result, there is a strong mechanical lithosphere of significant thickness. Extension of this strong layer gives rise to earthquakes, large-scale normal faulting, and the development of a

median rift valley. Unlike faster spreading rises where plate divergence is accommodated almost entirely by magmatic accretion, along slower spreading ridges the cumulative throw of seafloor normal faults (Macdonald & Luyendyk 1977) and the rate of seismic moment release (Solomon et al 1988) indicate that about 20% of plate divergence is accommodated by lithospheric stretching. Scenarios for segmentation of slow-spreading ridges (Crane 1985, Whitehead et al 1984, Schouten et al 1985) and recent bathymetric and gravity surveys (Sempere et al 1990, Lin et al 1990) suggest systematic variations in the thermal and mechanical properties of the lithosphere along a single ridge segment. Lithosphere near the magmatic center should be relatively hotter and mechanically weaker and should display evidence for more recent magmatism, whereas lithosphere more distant from the magmatic center should be cooler and mechanically stronger.

Several recent experiments have addressed the seismic velocity, density, or mechanical structure of the Mid-Atlantic Ridge and its variation within and between major ridge segments (Figure 7). These include conventional seismic refraction (Purdy & Detrick 1986), marine gravity (Kuo & Forsyth 1988, Lin et al 1990, Morris & Detrick 1991), multichannel seismic reflection (Detrick et al 1990), microearthquake location and delay time tomography (Toomey et al 1985, 1988; Kong et al 1992), and earthquake centroid depth determination from body waveform inversion (Huang et al 1986, Huang & Solomon 1988). An increasingly multidisciplinary focus on selected sites has greatly accelerated our understanding of the interrelations among axial magmatic, tectonic, and hydrothermal processes and of the systematics of axial segmentation.

MEDIAN VALLEY STRUCTURE: BATHYMETRY The median valley of the Mid-Atlantic Ridge is centered on an inner floor of variable width (5–15 km) that contains the neovolcanic zone and is bounded by a nested series of generally rotated, seismogenic, normal-fault blocks that rise outward to the crestal mountains. The width and relief of the median valley are typically 20–30 km and 2000–3000 m, respectively; although the relief may be as little as hundreds of meters and as great as 4000–5000 m. The range in the shape and relief of cross-axis profiles provides an indication of the variable thermal and mechanical structure along slow-spreading ridges.

High-resolution multibeam bathymetric maps of the Mid-Atlantic Ridge (Sempere et al 1990, Lin et al 1990) document the form of morphologic segmentation of slow-spreading ridges (Figure 8). Maxima in the along-axis depth profile coincide with spreading center discontinuities, such as transform faults or non-transform offsets of the neovolcanic zone, while minima are sited approximately midway between discontinuities.

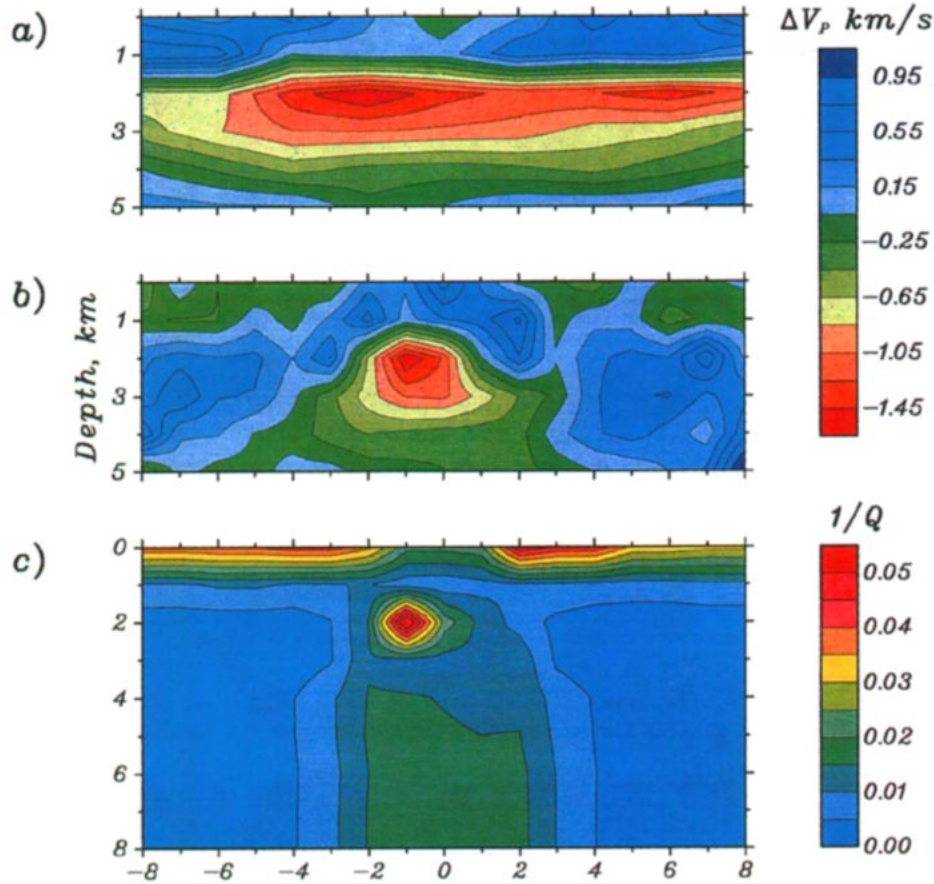

Figure 3 Vertical cross sections through the *P*-wave velocity (V_P) and attenuation (Q^{-1}) structures obtained by seismic tomographic imaging of the East Pacific Rise axis at 9°30′N (Toomey et al 1990, Wilcock et al 1991). (*a*) Along-axis section of the V_P structure 1 km to the west of the rise axis and passing through the center of the axial low-velocity volume. The colors represent departures of the three-dimensional model from the average one-dimensional, depth-dependent velocity structure; positive differences are faster than average, negative slower than average; 0.2 km/s contour interval. Two deviations from axial linearity (devals) occur at about −6 and 4 km range. (*b*) Cross-axis section of the V_P structure passing 2 km south of the experiment center. (*c*) Cross-axis section of apparent Q^{-1} structure. The two-dimensional structure was obtained by constrained, nonlinear tomographic inversion of *P*-wave spectral slope data along paths crossing the rise-axis 0–5 km south of the experiment center.

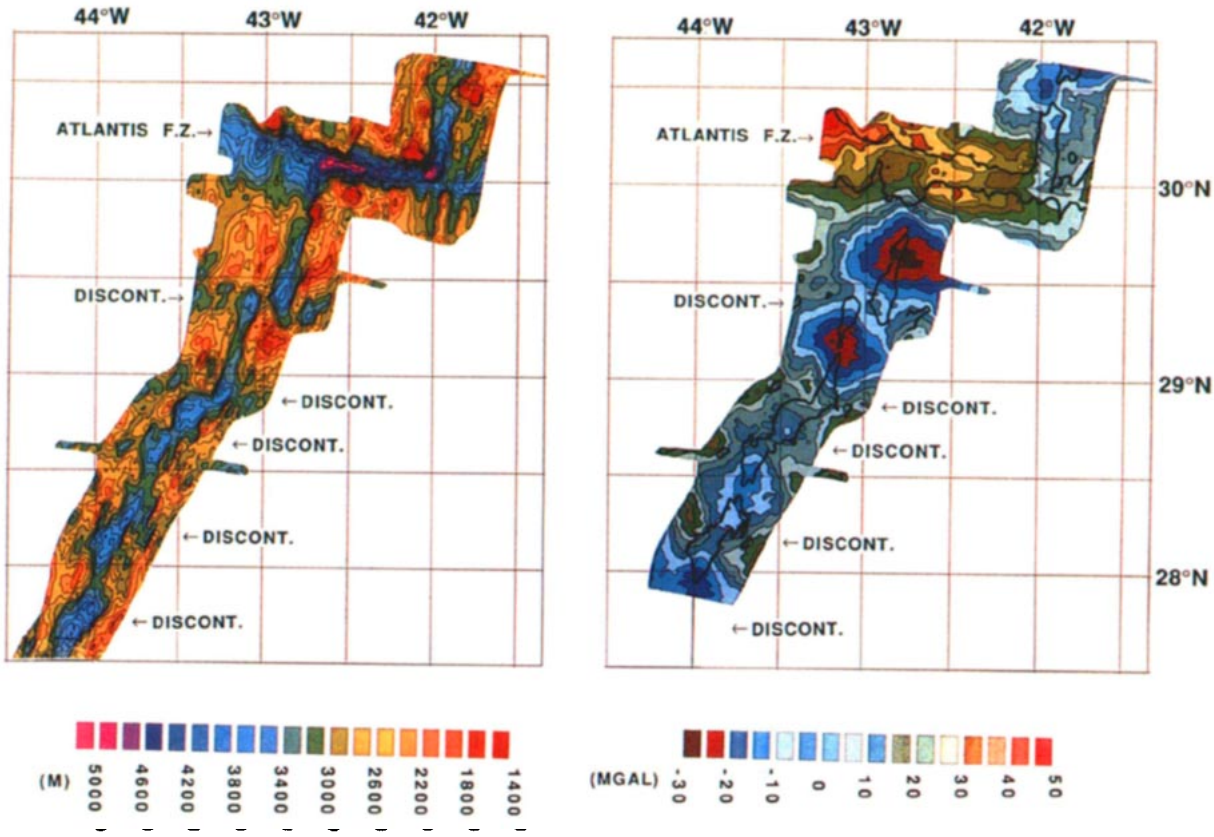

Figure 8 Sea Beam bathymetric map (*left*) and mantle Bouguer gravity anomaly map (*right*) of the Mid-Atlantic Ridge between about 28° and 31°N (from Lin et al 1990). The ridge axis is segmented into sections 20–80 km in length; gravity anomaly lows are centered over each segment. The contour interval is 200 m for bathymetry and 5 mgal for mantle Bouguer anomaly; the zero level for mantle Bouguer anomaly is arbitrary.

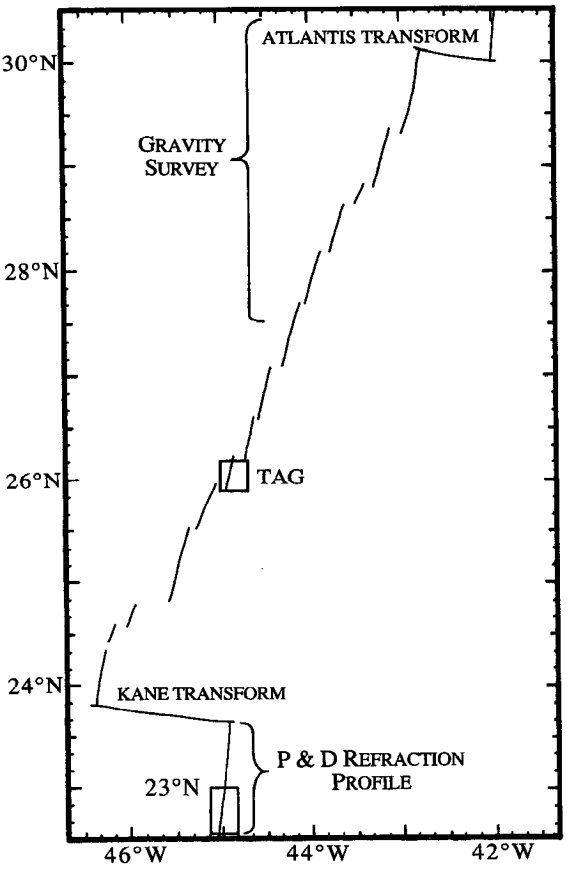

Figure 7 Sites of important geophysical experiments along the axis of the northern Mid-Atlantic Ridge, including the area of the gravity survey of Lin et al (1990), the micro-earthquake and two-dimensional tomography studies at 23°N (Toomey et al 1985, 1988) and 26°N (Kong et al 1992), and the refraction profile of Purdy & Detrick (1986) south of the Kane transform.

Segments are 20–90 km in length. The total along-axis relief within a segment generally increases with increased segment length.

The morphology of the median valley within a segment can be characterized as either narrow and shallow or broad and deep. These characteristics are thought to be thermally controlled, with the former indicating a relatively hot, more recently magmatically active segment and the latter a cooler, more tectonically active one. A single segment may be hour-glass-shaped in map view, with a narrow, shallow rift valley near its center and

a broader, deeper valley toward the distal ends, suggesting systematic intra-segment variability in thermal structure. It is not known whether the spectrum of along-axis bathymetry and segmentation observed in surveys to date fully characterize the range of styles of slow-spreading ridge systems.

ALONG-AXIS VARIATIONS: GRAVITY Gravity observations collected along the Mid-Atlantic Ridge provide further constraints on the physical characteristics of segmentation and suggest that magmatic accretion is focused at discrete locations near segment centers (Kuo & Forsyth 1988, Lin et al 1990, Morris & Detrick 1991). The gravity data, corrected for depth and constant crustal thickness to yield mantle Bouguer anomalies, show circular gravity lows centered near the midpoints of morphologically defined segments (Figure 8). The variations in density that accompany cooling of the oceanic lithosphere may account for some component of the cross-axis mantle Bouguer anomaly, but a thermal model consistent with only passive mantle upwelling does not account for the observed along-axis variations. The mantle Bouguer anomalies are more negative for longer ridge segments (Lin et al 1990); see Figure 9. The interpretation of the gravity anomalies is that magmatic accretion is focused near the center of a segment and that the vigor of magmatic activity at the midpoint of a segment increases with segment length.

Two specific hypotheses on the form of focused magmatic accretion have been proposed to explain the gravity anomalies (Lin et al 1990). The first attributes the heterogeneous density structure to along-axis variations in crustal thickness. Since the mantle Bouguer correction is calculated for a fixed crustal thickness, any departures from this structure will appear as an anomaly. Consequently, the mantle Bouguer anomaly pattern could arise from a relatively thick crust near the center of a ridge segment and relatively thinner crust near the segment ends. Alternatively, the along-axis gravity lows may arise from variations in upper-mantle density structure. In this hypothesis, the anomalous density structure is attributed to buoyancy-driven mantle upwelling. There are at least two sources of buoyancy: thermal expansion due to elevated temperature and the compositional buoyancy of depleted, relative to unmelted, mantle material. The two hypotheses are not mutually exclusive but rather constitute simple end-member models for anomalous density structure. Since hotter mantle would normally be expected to give rise to greater melt generation and thus greater crustal thickness, it is likely that the variations in along-axis gravity result from variations in both crustal and mantle structure. For both hypotheses mantle melt production is distinctly three-dimensional and focused near segment centers.

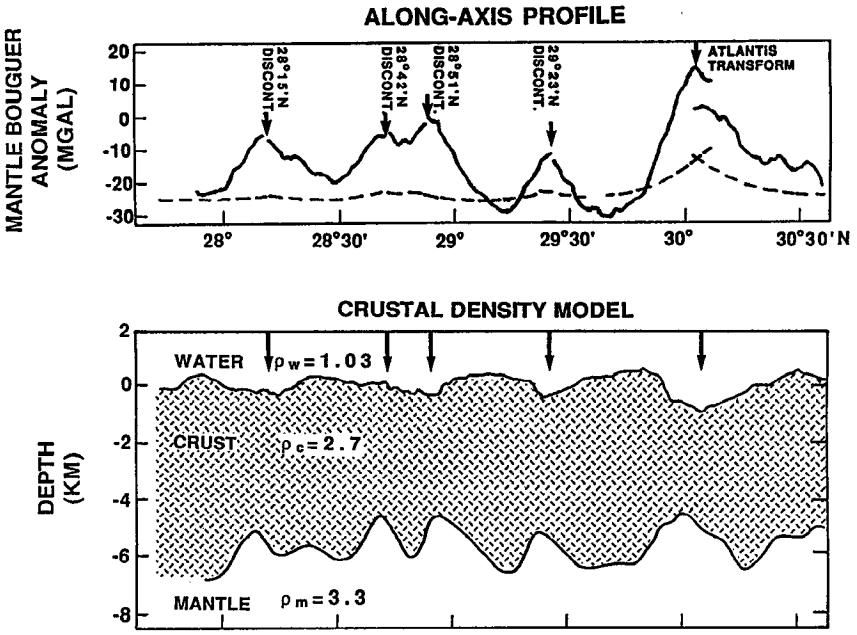

Figure 9 (*Top*) Along-axis profile (Lin et al 1990) of mantle Bouguer gravity anomaly (*solid line*) and the predicted anomaly (*dashed line*) for a model with fixed crustal thickness and the thermal structure given by a passive upwelling model for mantle flow (Phipps Morgan & Forsyth 1988). (*Bottom*) Along-axis bathymetry and crustal thickness for a model in which the entire mantle Bouguer anomaly is due to variations in crustal thickness (Lin et al 1990); the crust in this model is predicted to be thickest near the segment midpoints and thinnest at the segment ends.

ALONG-AXIS VARIATIONS: SEISMIC STRUCTURE AND SEISMICITY The nature of the seismic structure of the crust along the axis of a slow-spreading ridge, and of its variability within and between segments, is well illustrated by a seismic refraction line shot down a 120-km-long section of the axis of the Mid-Atlantic Ridge south of the Kane Fracture Zone (Purdy & Detrick 1986). For most of the length of the profile, the structure is similar to that of normal oceanic crust, with a well-defined Moho transition zone, a mantle *P*-wave velocity of about 8 km/s, and a normal crustal thickness of 6–7 km. Only a slightly low velocity to layer 3 distinguishes this structure from that of mature oceanic crust. Two significant along-axis structural changes, however, are noteworthy (Figure 10): a 10–15-km-wide zone of low velocities in the lower crust beneath an along-axis high, and a zone of complex structure marking the transition northward to thinner crust near the intersection of the median valley with the Kane transform. On the

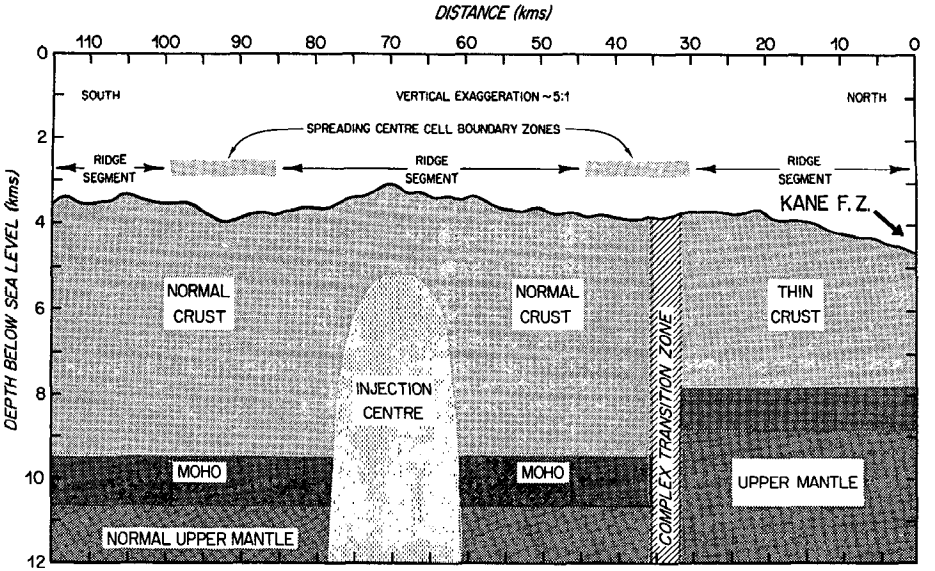

Figure 10 Schematic representation of crustal structure inferred from seismic refraction data along a 120-km-long section of the Mid-Atlantic Ridge axis south of the Kane Fracture Zone (from Purdy & Detrick 1986). On the basis of anomalously low velocities in the lower crust, the axial high near the midpoint of the central segment is interpreted to be the site of most recent injection of (now solidified) magma into the crust.

basis of along-axis bathymetry as well as structure, Purdy & Detrick (1986) interpret these two zones as marking the center and end, respectively, of a spreading center segment. At no location along the 120-km length of ridge was any evidence found for a significant body of molten or partly molten rock. A multichannel seismic reflection profile along the northern portion of the refraction line, including the site of a high-temperature hydrothermal field (ODP Leg 106 Scientific Party 1986), also failed to find evidence for a shallow intracrustal reflector that might be associated with a crustal magma body (Detrick et al 1990).

The distribution of earthquake hypocenters both across and along the median valley has important implications for the thermal and mechanical structure of a ridge segment. According to current models for segmentation, lithosphere near the ends of a segment should be thicker, tectonic stretching should be more important, and faulting should extend deeper than near segment midpoints. From the inversion of teleseismic *P* and *S* waveforms from 50 large earthquakes along slow-spreading ridge systems, Huang & Solomon (1988) showed that the maximum centroid depth, and thus the greatest extent of seismogenic faulting, increased systematically

with decreasing spreading rate. This result indicates a strong spreading-rate dependence to the maximum thickness of the mechanically strong lithosphere within the median valley inner floor, where the epicenters of the largest ridge earthquakes are located. Huang & Solomon (1988) and Lin & Bergman (1990) have shown further that there is a clear tendency for the largest earthquakes on slow-spreading ridges to occur near the ends of morphological segments.

Microearthquake experiments with networks of ocean-bottom seismometers and hydrophones permit the delineation of patterns of faulting within a segment in much greater detail than with only teleseismic data. One such microearthquake study, near 23°N, was sited in an along-axis deep at the southern end of a ridge segment approximately 40 km in length (Toomey et al 1985, 1988); the segment is depicted in the center of Figure 10. Earthquakes occurred as deep as 8 km beneath the inner floor, indicating brittle failure throughout the crustal column and probably into the uppermost mantle. Fault-plane solutions for several groups of events indicated normal faulting mechanisms, consistent with lithospheric stretching. In combination with observations of the rate of occurrence and typical fault slip of large earthquakes on this segment (Huang et al 1986), an asymmetry in the inner floor indicated by multibeam bathymetry (Detrick et al 1984), and the nearly normal oceanic crustal structure indicated by seismic refraction (Purdy & Detrick 1986), the microearthquake data imply (Figure 11) that this median valley deep has undergone horizontal extension without axial magmatism for approximately the last 10^4 years (Toomey et al 1988).

A second microearthquake experiment was located near 26°N, at an along-axis high near the midpoint of a ridge segment also approximately 40 km in length (Kong et al 1992). In contrast to the magmatically quiescent, comparatively cooled crust beneath the along-axis deep at 23°N, the axial high of the ridge segment at 26°N is the site of a black-smoker hydrothermal vent field (Rona et al 1986). Within the inner floor, the maximum focal depth of events beneath the region of the along-axis high was less than that of earthquakes beneath the along-axis deep 15 km to the south (Figure 12), consistent with a hotter crust and thinner mechanical lithosphere beneath the high. The fault plane solutions of grouped events indicated diverse source mechanisms and a variable state of stress.

Analysis of the travel-time residuals of *P* waves recorded on seafloor networks also permits tomographic imaging of the local seismic velocity structure of the crust in the vicinity of the network. At 23°N the two-dimensional seismic structure across the median valley inner floor at the site of the axial deep shows that the modest decrease in the layer 3 velocity indicated in the along-axis refraction results (Purdy & Detrick 1986) is

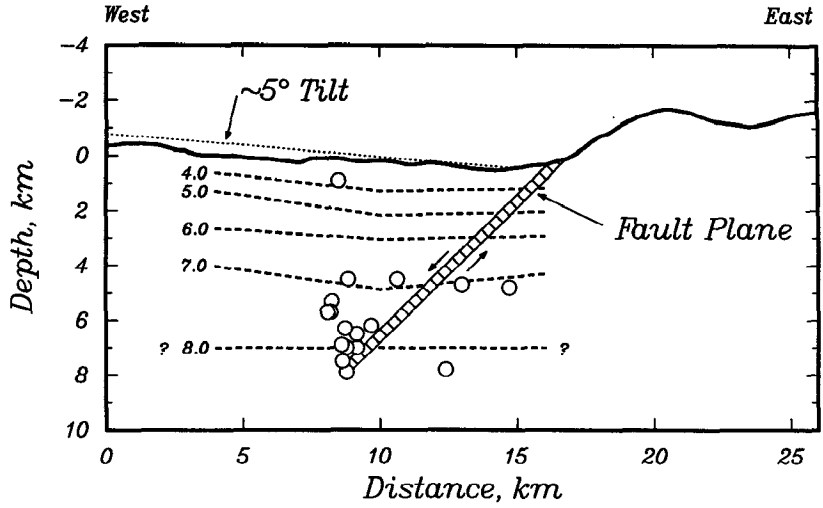

Figure 11 Cross-axis vertical section of the Mid-Atlantic Ridge median valley along-axis deep near 23°N, showing microearthquake hypocenters (*circles*) and contours of *P*-wave velocity (in km/s) obtained from two-dimensional delay-time tomography (Toomey et al 1988). Bathymetry is from the Sea Beam survey of Detrick et al (1984). A conjectural fault plane for recent large ($m_b > 5$) earthquakes, consistent with fault geometry and dimensions inferred from body waveform inversion (Huang et al 1986), is shown as a continuation at depth of the fault making up the steep eastern inner wall of the median valley. If the full rate of plate separation were accommodated by slip on that fault over 10^4 yr, the fault throw and the observed eastward tilt of the inner floor can both be matched.

largely eliminated by an age of a few hundred thousand years (Figure 11). A tomographic inversion for two-dimensional structure along the inner floor axis at 26°N shows anomalously low mid-crustal velocities beneath the along-axis high (Figure 12). Toward the axial deep at the southern end of this ridge segment the seismic structure is comparable to normal oceanic crustal structure, similar to the axial deep near 23°N. This along-axis variation is consistent with the hypothesis that crustal accretion is focused near the center of the ridge segment (Kong et al 1992).

The relationships documented among segment length, axial relief, and mantle Bouguer gravity anomaly minimum (Lin et al 1990) suggest that the ridge segments near 23°N and 26°N are architecturally similar. The two microearthquake experiments, together with teleseismic analysis of large earthquakes and seismic refraction data, may thus begin to characterize the intra-segment seismic structure of a 40-km-long ridge segment on a slowly spreading ridge. Near the segment center the mechanically strong lithosphere is only a few kilometers thick and the tectonic state is

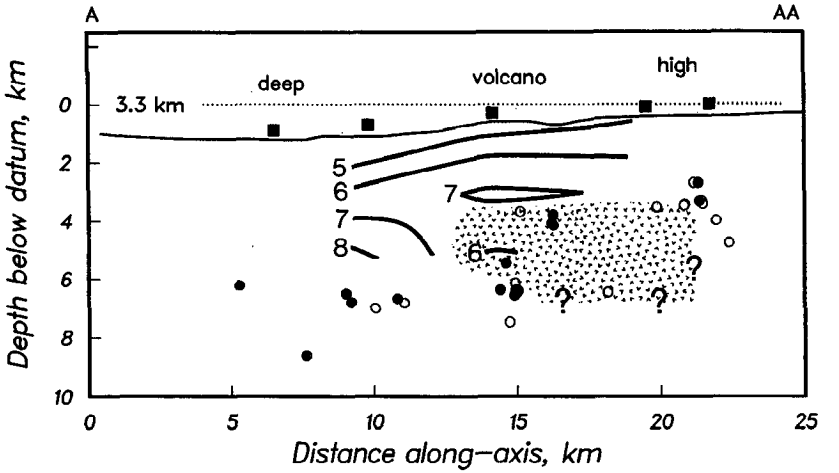

Figure 12 Along-axis vertical section of the Mid-Atlantic ridge median valley near 26°N, showing microearthquake hypocenters (*circles*, filled where the locations were constrained by one or more *S*-wave arrival times) and contours of *P*-wave velocity (in km/s) obtained from two-dimensional delay-time tomography (Kong et al 1992). Filled squares show the locations of ocean-bottom seismic stations. The stippled area shows the location of a region of low velocities imaged in the mid to lower crust beneath the axial high and black-smoker hydrothermal field; the lower and northern limits of this anomaly are uncertain. The low velocities are attributed to elevated temperatures at the site of the most recent crustal injection of (now solidified) magma along this ridge segment.

highly variable, reflecting a mix of extension and thermal stress accompanying rapid cooling (Kong et al 1992), while the segment ends are characterized predominantly by ongoing extension and seismogenic faulting extending to the base of the crust (Toomey et al 1988, Huang & Solomon 1988).

Implications for Crustal Formation

Seismic data on mid-ocean ridge crustal structure indicate that the axial magma chamber departs significantly from the earlier predictions from ophiolites (e.g. the lower panel of Figure 1) that the chamber would be large and nearly steady state. No magma body has been found along slow-spreading ridges despite a concerted search. The axial magma body along fast-spreading rises is only a thin sill, perhaps typically no more than 1 km in width and 100 m or less in thickness (Kent et al 1990). The diagnostic AMC reflector was not seen along nearly 40% of the northern East Pacific Rise axis imaged by multichannel reflection profiling (Detrick et al 1987), indicating that even the thin magma lens is not a steady-state feature at

fast spreading rates. Two inferences may be made from these findings. The first is that the process of cooling and solidifying magma delivered to the upper crust along the axial neovolcanic zone must occur on a time scale comparable to (at fast spreading) or faster than (at slow spreading) that of magma delivery. To be this efficient the cooling of the axial crust must occur dominantly by hydrothermal circulation. The second inference is that the transport of magma to the axial crust must be time-dependent and spatially variable. The spatial variability applies equally to the flow regime in the ridge upper mantle responsible for magma generation. The possibility of a large axial magma chamber remains open, but such a feature would be transient and is likely to be a rare event in space and time.

The relationship between the vertical structure of oceanic crust and the evolution of the axial magma chamber also requires modification from the predictions of early ophiolite-based models. Although the upper crustal lithostratigraphy of oceanic crust is similar to the volcanic basalts and sheeted dikes of the ophiolite model (Anderson et al 1982) and such rocks are capable of being emplaced above the modest magma bodies imaged by seismic experiments along fast-spreading rises, the detailed mechanism of emplacement of layer 3 remains to be completely explained. One possibility is that the axial lower crust is episodically filled with a transient magma chamber capable of differentiation of a basal cumulate layer—much like the ophiolite model but with nearly complete solidification—even at fast spreading rates, before a new large batch of magma is again injected into the crust. This possibility would be considerably strengthened were a large magma chamber discovered along at least one ridge segment. A second possibility is that the axial magma chamber never significantly exceeds the dimensions or crustal depth of the magma lenses imaged seismically along the northern East Pacific Rise. Emplacement of the lower 4–5 km of crust must then occur by some form of solid-state flow downward and outward from the magma lens. This scenario raises the question as to how a seismically sharp crust-mantle transition can be consistently formed at the characteristic Moho depth for oceanic crust. The trapping of melt within sills at the base of the crust (Garmany 1989) may play a role in the formation of Moho structure.

Seismic and mechanical structure clearly are segmented in a manner related to other measures of ridge-axis segmentation, but the scales of segmentation within the crust are incompletely defined and the relationship of these scales to causative processes is not established. At the longest scales of segmentation, between major transform faults, the lithosphere is clearly exerting an influence on the pattern of mantle upwelling and melt generation. Along slow-spreading ridges, there appears to be a systematic

variation along a segment in the thickness of the strong mechanical layer in a sense consistent with the hypothesis that the delivery of heat and magma from the mantle is concentrated at the segment center. At the 10-km scale of morphological segmentation along fast-spreading rises, the coincidence of intracrustal seismic and thermal segment boundaries with morphological boundaries also suggests control by magmatic processes. Thus the dynamics of the coupled mantle-melt system are of prime importance for some segmentation scales.

RECENT RESULTS ON RIDGE UPPER MANTLE STRUCTURE

The seismic velocity and density of the upper mantle beneath mid-ocean ridges are functions of local temperature and bulk composition. The distribution of these quantities are in turn related to patterns of mantle flow, the extent of mantle melt extraction, and mantle chemical heterogeneity. The seismic velocity of oceanic mantle material is also known to be anisotropic. The sense and magnitude of this anisotropy provide important constraints on the processes of lithospheric spreading and mantle dynamics. Considerable progress has recently been made toward defining the laterally heterogeneous seismic velocity structure of ocean-ridge mantle from tomographic inversions of the phase and group velocities of long-period surface waves and the travel times of long-period body waves. For a review of many of the techniques used in such studies and a summary of recent findings see Romanowicz (1991).

The most prominent lateral variation in structure of the oceanic upper mantle is that associated with the cooling and aging of oceanic lithosphere. Mid-ocean ridge axes are resolved as regions of generally low upper-mantle velocities in global and regional tomographic inversions (Woodhouse & Dziewonski 1984; Grand 1987; Zhang & Tanimoto 1989, 1991; Montagner & Tanimoto 1990), and an age-dependence has been documented for both surface-wave phase and group velocities (Leeds et al 1974; Forsyth 1975, 1977; Yoshii 1975; Mitchell & Yu 1980; Montagner & Jobert 1983; Nishimura & Forsyth 1985, 1988) and the travel times of steeply incident body waves (Duschenes & Solomon 1977, Girardin 1980, Kuo et al 1987, Woodward & Masters 1991, Sheehan & Solomon 1991). Examples of this age dependence are shown in Figures 13 and 14.

An important question is whether the age dependence of seismic velocity is entirely an effect of lithospheric cooling or also contains a contribution from the sublithospheric mantle. Zhang & Tanimoto (1991) find that the variation of Love wave phase velocity versus age shown in Figure 13 can

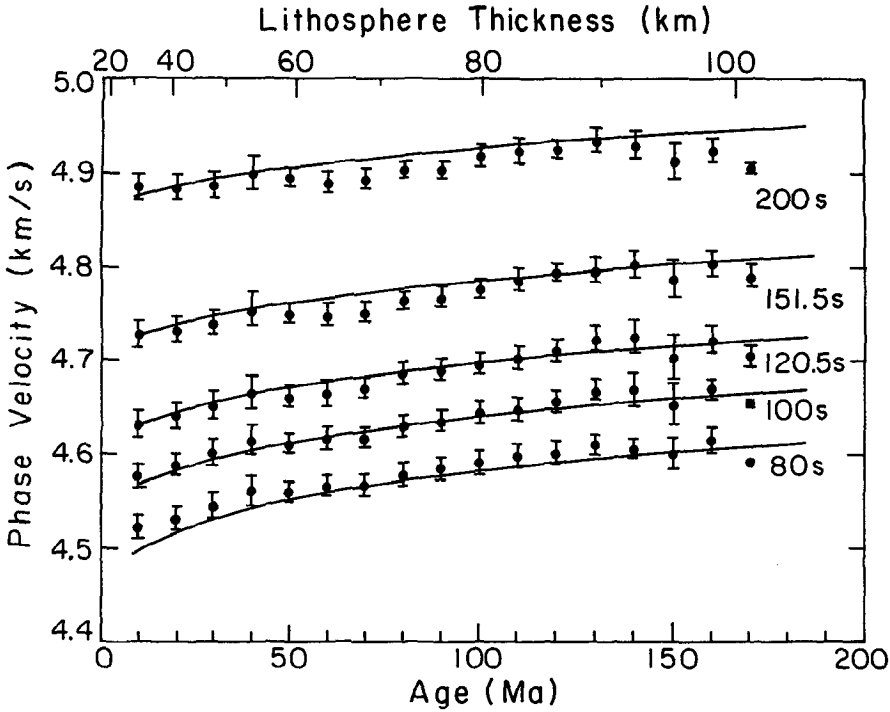

Figure 13 Love wave phase velocity versus seafloor age and wave period in the Pacific Ocean (from Zhang & Tanimoto 1991). Error bars denote one standard deviation. The solid lines are the predicted variations for a model in which a high-velocity lithosphere thickens in proportion to the square root of age.

be explained entirely by the thickening of oceanic lithosphere with age, as long as the thickness is proportional to the square root of seafloor age, even out to ages in excess of 100 Ma. A similar finding has been reported from efforts to model pure-path Rayleigh wave phase velocities (e.g. Leeds et al 1974), although other workers (Yoshii 1975, Forsyth 1977) report that some increase with age in the shear velocity of the underlying asthenosphere is also required. The *PP-P* and *SS-S* differential travel times, plotted at the seafloor age of the surface-reflected phase (*PP* or *SS*) and averaged by age as in Figure 14 (from Woodward & Masters 1991), also show an approximately linear decrease with square root of age out to ages in excess of 100 Ma, although Sheehan & Solomon (1991) note an apparent departure from the linear relation for ages greater than 100 Ma in the North Atlantic. The *SS-S* differential travel time that would result from a

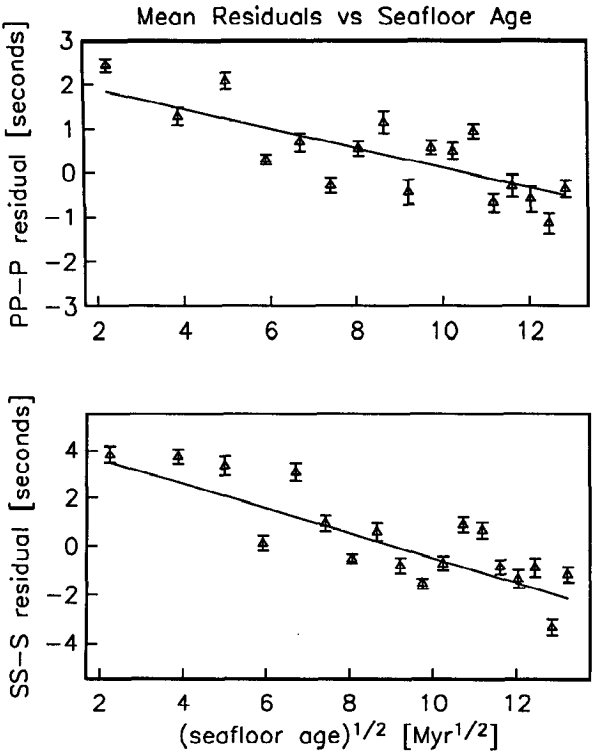

Figure 14 *PP-P* and *SS-S* differential travel-time residuals in oceanic regions versus the square root of age of the seafloor at the bounce point of the surface-reflected phase (*PP* or *SS*) (from Woodward & Masters 1991). Each point shown is an average of about 100 measurements; error bars denote one standard deviation. Most of the variation depicted is due to cooling of the oceanic lithosphere as it spreads from the ridge axis.

standard lithospheric plate cooling model (Parsons & Sclater 1977) and a constant partial derivative of shear wave velocity with temperature (-0.6 m/s K^{-1}) provides a good fit to the data for the North Atlantic for ages less than 100 Ma (Sheehan & Solomon 1991). At the very long wavelengths (typically several thousand kilometers and greater) represented by upper mantle tomographic models, however, there is evidence in the results of inversions of both surface wave or normal mode data and body wave travel times for low-velocity volumes extending as deep as 300–400 km beneath the crestal regions of actively spreading mid-ocean ridges (Woodhouse & Dziewonski 1984, Grand 1987, Zhang & Tanimoto 1989). Most likely these low velocities are a reflection of temperatures that are greater

than average for those mantle depths and indicate that mantle upwelling associated with plate divergence extends to at least 300–400 km depth.

If the age-dependent lateral variation in seismic velocity associated with lithospheric cooling is removed from surface wave velocities or differential travel times depicted in map view, then the residual velocities or times are measures of one or more additional components of lateral heterogeneity. Sections of the global ridge system that are extremes in residual Rayleigh wave velocities are the Reykjanes Ridge (anomalously slow, Girardin & Jacoby 1976) and the Southeast Indian Ocean Ridge in the vicinity of the Australian-Antarctic discordance (anomalously fast, Forsyth et al 1987); the axes of these ridge sections are also, respectively, anomalously shallow and deep and likely reflect characteristic mantle temperatures significantly hotter and colder, respectively, than average. Sheehan & Solomon (1991) have documented variations in age-corrected *SS-S* differential travel times at wavelengths of 1000 to 7000 km along the axis of the Mid-Atlantic Ridge; an along-axis variation in the phase velocity of 100-s Love waves (Zhang & Tanimoto 1991) shows a generally similar pattern. The variations in *SS-S* travel-time residuals show strong qualitative correlations with along-axis variations in bathymetry and geoid height (Figure 15) and are likely to be the result of long-wavelength variations in the characteristic temperature and bulk composition of the ridge-axis mantle. Sheehan & Solomon (1991) have formulated a procedure to invert jointly the residual *SS-S* differential travel time, bathymetry, and geoid profiles for lateral variations in upper mantle temperature and Mg # [the molar ratio MgO/(MgO+FeO)]. Temperature and Mg # can be distinguished, in principle, because while an increase in temperature results in a decrease in both seismic velocity and bulk density, an increase in Mg # decreases density but increases seismic wave speed. The resulting models of horizontal variation in mantle temperature and composition along the Mid-Atlantic Ridge (e.g. Figure 16) compare favorably with independent estimates from the composition and geothermometry of peridotites (Michael & Bonatti 1985, Bonatti 1990) and the depth interval of melting implied by the FeO content of mantle-derived basalts (Klein & Langmuir 1989) dredged from along the ridge axis. If the composition of the mantle at several hundred kilometers depth were constant along a mid-ocean ridge, then the characteristic upper mantle temperature should be strongly related to mantle Mg #. A higher temperature should yield a greater extent of mantle melting, and since melt extraction from the mantle is thought to be an efficient process, the residuum should be enriched in MgO relative to less melted mantle (McKenzie 1984). Characteristic temperature and Mg # are not strongly correlated in Figure 16, however; nor are there known to be along-axis variations in crustal thickness that would be

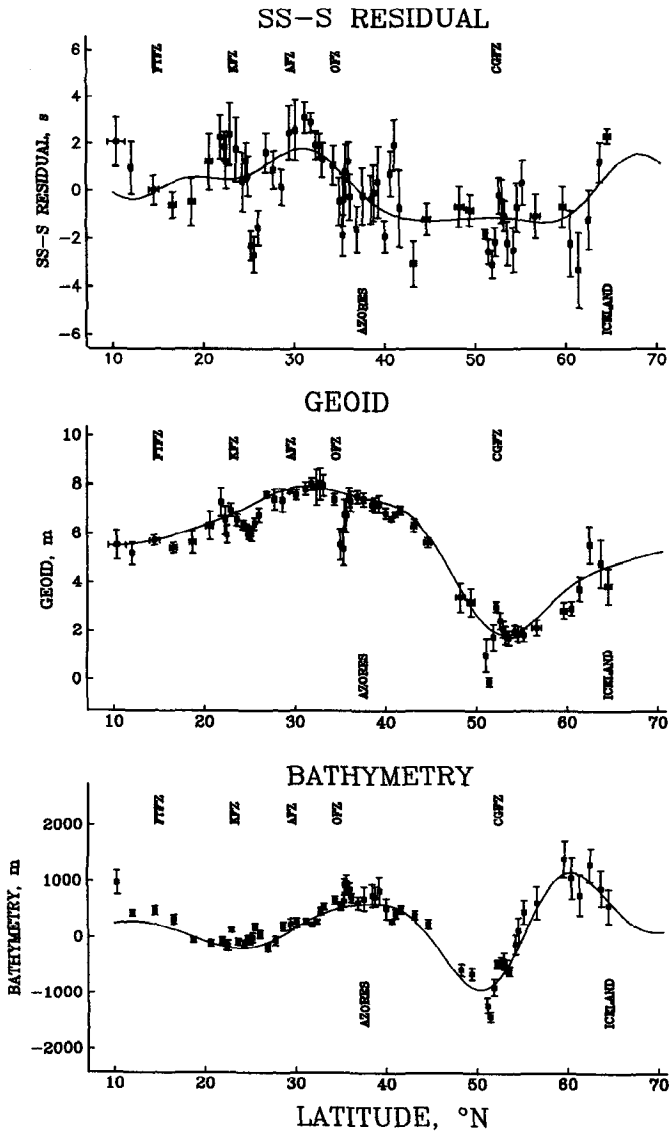

Figure 15 Comparative profiles of age-corrected *SS-S* travel-time residual, bathymetry, and geoid height along the Mid-Atlantic Ridge (from Sheehan & Solomon 1991). All three data types have been high-pass filtered. The points shown are moving averages of 10 adjacent data points, taken for all data types at the *SS*-wave bounce locations; error bars denote standard errors of the means. The solid lines represent filtered versions of the depicted observations, containing only the wavelengths (1400 to 7100 km) used in the inversions for along-axis variations in mantle temperature and composition.

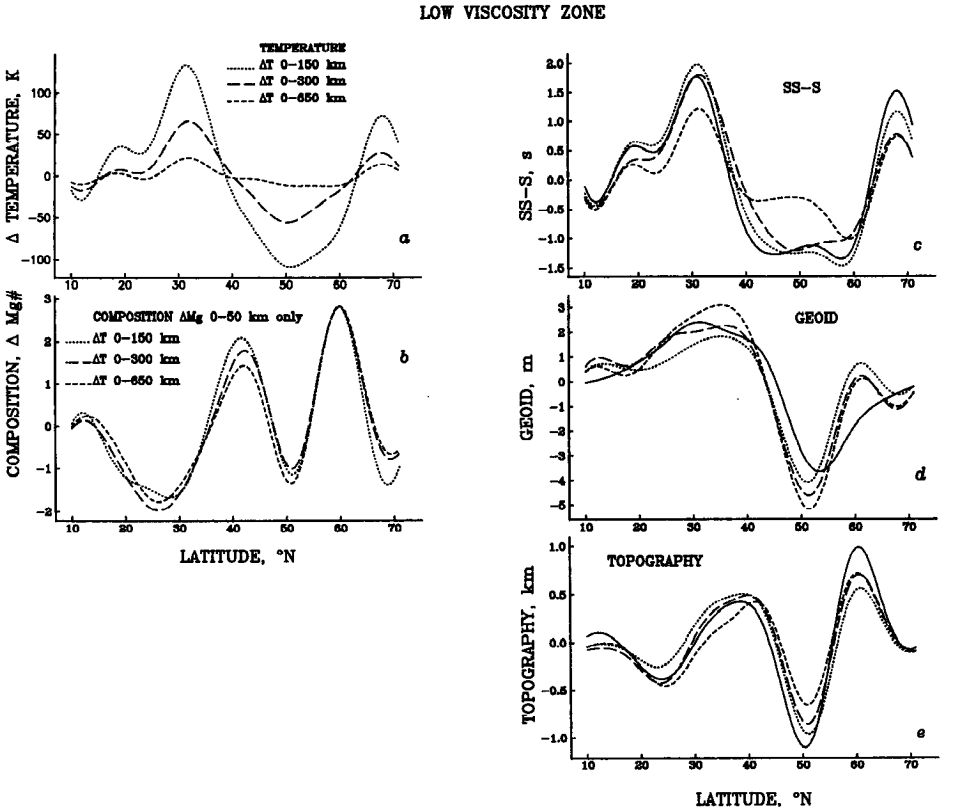

Figure 16 Results of the combined inversion of *SS-S* travel-time residuals, bathymetry, and geoid height for along-axis variations in upper mantle temperature and composition (from Sheehan & Solomon 1991). Composition is parameterized in terms of Mg #. The solutions include the dynamic effects of variations in density; the viscosity structure is taken to consist of a 40-km-thick high-viscosity lid, a low-viscosity zone extending from the base of the lid to a depth of 200 km, and a constant-viscosity underlying mantle. (*a*) Three solutions for along-axis temperature variations: Temperature perturbations are variously constrained to be uniform over 0–150 km depth (*dotted line*), 0–300 km depth (*long dashed line*) or 0–650 km depth (*short dashed line*). (*b*) The corresponding solutions for along-axis composition variations, constrained to occur over the depth interval 0–50 km. (*c*) Observed (*solid line*) and predicted along-axis profiles of *SS-S* travel-time residual. The "observed" profile is the filtered profile of Figure 15. (*d*) Observed and predicted along-axis geoid height profiles. (*e*) Observed and predicted along-axis bathymetry profiles.

expected to result, under the assumption of passive upwelling at ridges (McKenzie 1984), from the along-axis differences in temperature depicted in the figure. Possible explanations for these departures from the expectations of simple models include long-wavelength variations in mantle chemistry unrelated to degree of melt extraction, variations in the volatile content of the melt-generating zones, or a component of dynamic upwelling driven by melting-induced changes in buoyancy (Sheehan & Solomon 1991, Forsyth 1992).

An important element of seismic structure potentially relatable to mantle flow and lithospheric emplacement processes is the anisotropy of seismic velocity in the oceanic upper mantle. As noted above, an azimuthal anisotropy extends throughout most, if not all, of the mantle portion of oceanic lithosphere. In principle, the accumulated strain induced by mantle convective flow should also impart a bulk anisotropy to the sublithospheric mantle, at least that part of the mantle within the stability field of olivine (McKenzie 1979, Ribe 1989). Two forms of anisotropy are potentially indicative of mantle convective flow directions: differences in velocity between horizontally and vertically propagating waves (polarization anisotropy) and variations in velocity with azimuth. Variations in polarization anisotropy can, in principle, distinguish regions of upwelling and downwelling from those areas dominated by horizontal flow, and azimuthal anisotropy indicating a fast direction distinct from the direction of seafloor spreading at the time of formation of the overlying crust (sometimes called the fossil spreading direction) can be a signature of the predominant direction of horizontal asthenospheric flow. Several seismological efforts to detect these forms of anisotropy have been reported. Kuo et al (1987) report that *SS-S* differential travel times in the North Atlantic show a dependence on the azimuth of the *SS* path at the surface-reflection point, with the pattern consistent with a N-S orientation to the olivine *a*-axis in the sublithospheric mantle; they interpreted this pattern as an indication of the orientation of asthenospheric flow in the region (Hager & O'Connell 1979). Neither Woodward & Masters (1991) nor Sheehan & Solomon (1991) found a consistent pattern of significant azimuthal anisotropy in a larger set of *SS-S* times from the North Atlantic, however; Woodward & Masters (1991) resolved an azimuthal dependence of *SS-S* times in the Pacific consistent with the fast direction in the mantle being oriented parallel to the direction of absolute plate motion, but they could not eliminate the possibility that the pattern was an effect of geographic bias in the paths within distinct ranges in azimuth.

Surface waves are sensitive to both polarization and azimuthal anisotropy. Nishimura & Forsyth (1989) inverted Love and Rayleigh wave phase velocities in the Pacific to determine the age and depth dependence

of both polarization and azimuthal anisotropy. They found that the ratio of horizontal to vertical shear wave velocity increased from a minimum at young ages (0–4 Ma) to a steady value at ages greater than 20 Ma; they interpreted this result as evidence for dominantly vertical flow beneath the ridge axis. They found that the azimuthal anisotropy, when referenced to the fossil spreading direction, was strongest in regions less than 80 Ma in age, where the effect was a maximum between 25 and 100 km depth but persisted to 200 km depth; since the lithosphere does not extend as deep as 200 km, they interpreted this result as indicating a contribution from asthenospheric flow, which in the young regions of the eastern Pacific is thought to be nearly parallel to the local fossil spreading direction. In regions older than 80 Ma, the azimuthal anisotropy appears to be confined to depths less than 50 km, i.e. less than the thickness of the lithosphere; since this result is, at face value, contrary to both the prevailing model for anisotropy of the mantle lithosphere and evidence from refraction studies (Shimamura 1984), Nishimura & Forsyth (1989) interpreted this result as due to the partial cancellation of lithospheric anisotropy by the differently oriented azimuthal anisotropy of the asthenosphere in the western Pacific.

OUTSTANDING ISSUES AND FUTURE DIRECTIONS

Geophysical experiments designed to characterize the structure of mid-ocean ridges have considerably sharpened the hypotheses for the relationships among plate separation, mantle flow, melt generation, magma transport, and formation of oceanic crust, but these first experiments have, of necessity, been focused on limited areas and scales. Surface wave, normal mode, and long-period body-wave techniques are yielding new results on the oceanic mantle on horizontal scales of 10^3–10^4 km and vertical scales of 10^2 km, while active marine seismic experiments are illuminating the oceanic crust at horizontal scales of 1–10 km and vertical scales of 0.1–1 km. The intermediate horizontal and vertical scales remain important targets of future work. Further, it is well to remember that even the most revealing high-resolution seismic studies are only of local areas, and while some generalizations can be made from regional information such as bathymetry and gravity, most of these generalizations await testing with further, carefully selected high-resolution experiments.

One of the most promising directions for future seismic investigation of ridge processes is to elucidate the structure of the uppermost mantle beneath ridges on a scale sufficient to infer some of the characteristics of mantle flow and melt generation. These topics, heretofore largely in the

realm of theoreticians and numerical modelers, are amenable to study through the three-dimensional, anisotropic *P* and *S* wave velocity structure of the ridge upper mantle. The temperature variations associated with upwelling should have direct effects on bulk seismic velocities, and the shearing accompanying flow should yield diagnostic patterns of anisotropy. Beyond the hint from the age dependence of surface wave polarization for ages less than 20 Ma, there is not yet direct seismic confirmation of theoretical expectations that the zone of mantle upwelling and melt generation beneath ridges is of order 100 km in width, much less of various hypotheses advanced to account for the remarkable narrowing by some two orders of magnitude of the zone of the ascending melt into the ~1-km-wide neovolcanic zone (e.g. Phipps Morgan 1987, Scott & Stevenson 1989). What is required experimentally is a passive network of broad-band ocean bottom seismometers situated for one year or more astride a mid-ocean ridge. A combination of body-wave delay time tomography and inversion of surface wave dispersion data can yield two- and three-dimensional images of seismic velocities. Shear wave splitting and azimuthal and polarization anisotropy of surface waves can be used to infer the form of preferred crystal alignment in the mantle and its variation across the zone of upwelling. There is the possibility as well of detecting and characterizing the distribution of zones of melt within the upwelling mantle from the potentially strong effect of any melt fraction on the velocities and attenuation of seismic waves.

The relationship among the various scales of along-axis variability in seismic characteristics and the segmentation of axial processes remains to be explored, particularly the intermediate scales between the 1000-km variation resolvable with surface waves and global tomographic techniques and the 10-km scale addressible with an ESP profile or a crustal tomography experiment. These intermediate scales are those most likely to reflect dynamics of the mantle-melt system. Determination of along-axis variations in the seismic properties of the lowermost crust or uppermost mantle might reveal the nature of variations at this intermediate scale and their connection to other measures of segmentation. Good vertical resolution at these depths will pose a challenge. As with the shallow crust, a combination of seismic techniques probably offers the greatest promise for insight.

The detailed evolution from crustal-level melt to solid oceanic crust, including the important time scales for magma replenishment, solidification, and subsolidus deformation, is not understood. While theoretical, laboratory, petrological, and geochemical analyses of this problem all warrant pursuit, additional seismic experiments addressing this topic can be envisioned. For example, the different states of the magma lenses at 9°

and 13°N indicated by analysis of reflected waves (Harding et al 1989, Vera et al 1990) raise the possibility that systematic mapping of the reflection coefficient of the AMC reflector at near-normal incidence and as a function of range might reveal relationships among magma state, hydrothermal activity, recency of axial volcanism, or other measures of along-axis variability that would help to constrain the controlling processes and their time scales.

At slow spreading rates, the relation between segment length and such measures of mantle upwelling strength as axial depth minimum and mantle Bouguer anomaly magnitude (Lin et al 1990) have not been tested with seismic experiments. Microearthquake experiments designed to map the thickness of the mechanically strong lithosphere and to image the seismic velocity structure in three dimensions with passive seismic tomography should be conducted along slow-spreading ridge segments of a variety of lengths and cross-axis morphology. Because no axial magma body has yet been imaged along slow-spreading ridges, particular attention should be devoted during and after such experiments to any detected volumes of significantly lower than average crustal velocity.

The interpretation of both recently completed and future seismic experiments will benefit substantially from further laboratory measurements of seismic properties of crustal and mantle rocks at a range of pressures, temperatures, and frequencies appropriate to the oceanic crust and upper mantle. Particularly important will be measurements of P and S wave velocity and attenuation in partially molten mantle material, partially crystalline basaltic melt, and mostly crystalline gabbroic mush. Such measurements are critical to the eventual tracking of melt, by geophysical observation, from initial mantle generation to final crustal solidification.

ACKNOWLEDGMENTS

We thank Joe Cann, Dave Caress, Bob Detrick, Rachel Haymon, Jian Lin, G. M. Purdy, Emilio Vera, Bob Woodward, and Yu-Shen Zhang for copies of figures from their publications. Preparation of this review was supported by the National Science Foundation under grants EAR-9004750, OCE-9000177, and OCE-9106233, the Office of Naval Research under grants N00014-89-J-1257 and N00014-91-J-1216, and the National Aeronautics and Space Administration under grant NAG 5-814.

Literature Cited

Anderson, R. N., Honnorez, J., Becker, K., Adamson, A. C., Alt, J. C., et al. 1982. DSDP hole 504B, the first reference section over 1 km through layer 2 of the oceanic crust. *Nature* 300: 589–94

Bonatti, E. 1990. Not so hot "hot spots" in the oceanic mantle. *Science* 250: 107–11

Bratt, S. R., Purdy, G. M. 1984. Structure and variability of oceanic crust on the

flanks of the East Pacific Rise between 11° and 13°N. *J. Geophys. Res.* 89: 6111–25
Bratt, S. R., Solomon, S. C. 1984. Compressional and shear wave structure of the East Pacific Rise at 11°20′N: Constraints from three-component ocean-bottom seismometer data. *J. Geophys. Res.* 89: 6095–110
Bryan, W. B., Moore, J. G. 1977. Compositional variations of young basalts in the Mid-Atlantic Ridge rift valley near lat 36°49′N. *Bull. Geol. Soc. Am.* 88: 556–70
Burnett, M. S., Caress, D. W., Orcutt, J. A. 1989. Tomographic image of the magma chamber at 12°50′N on the East Pacific Rise. *Nature* 339: 206–8
Butler, R. 1985. Anisotropic propagation of P- and S-waves in the western Pacific lithosphere. *Geophys. J. R. Astron. Soc.* 81: 89–101
Cann, J. R. 1974. A model for oceanic crustal structure developed. *Geophys. J. R. Astron. Soc.* 39: 169–87
Caress, D. W., Burnett, M. S., Orcutt, J. A. 1992. Tomographic image of the axial low velocity zone at 12 50′N on the East Pacific Rise. *J. Geophys. Res.* In press
Casey, J. F., Dewey, J. F., Fox, P. J., Karson, J. A., Rosencrantz, E. 1981. Heterogeneous nature of oceanic crust and upper mantle: A perspective from the Bay of Islands ophiolite complex. In *The Sea*, Vol. 7, ed. C. Emiliani, pp. 305–38. New York: Wiley-Interscience
Casey, J. F., Karson, J. A. 1981. Magma chamber profiles from the Bay of Islands ophiolite complex. *Nature* 292: 295–301
Christensen, N. I., Salisbury, M. H. 1975. Structure and constitution of the lower oceanic crust. *Rev. Geophys. Space Phys.* 13: 57–86
Crane, K. 1985. The spacing of rift axis highs: Dependence upon diapiric processes in the underlying asthenosphere? *Earth Planet. Sci. Lett.* 72: 405–14
Detrick, R. S., Buhl, P., Vera, E., Mutter, J., Orcutt, J., Madsen, J., Brocher, T. 1987. Multi-channel seismic imaging of a crustal magma chamber along the East Pacific Rise. *Nature* 326: 35–41
Derick, R. S., Fox, P. J., Kastens, K., Ryan, W. B. F., Mayer, L., Karson, J. A. 1984. Sea Beam survey of the Kane Fracture Zone and the adjacent Mid-Atlantic Ridge rift valley. *Eos, Trans. Am. Geophys. Union* 65: 1006 (Abstr.)
Detrick, R. S., Mutter, J. C., Buhl, P., Kim, I. I. 1990. No evidence from multichannel reflection data for a crustal magma chamber in the MARK area on the Mid-Atlantic Ridge. *Nature* 347: 61–64
Duschenes, J. D., Solomon, S. C. 1977. Shear wave travel-time residuals from oceanic earthquakes and the evolution of oceanic lithosphere. *J. Geophys. Res.* 82: 1985–2000
Forsyth, D. W. 1975. The early structural evolution and anisotropy of the oceanic upper mantle. *Geophys. J. R. Astron. Soc.* 43: 103–62
Forsyth, D. W. 1977. The evolution of the upper mantle beneath mid-ocean ridges. *Tectonophysics* 38: 89–118
Forsyth, D. W. 1992. Geophysical constraints on mantle flow and melt generation beneath mid-ocean ridges. In *Mantle Flow, Melt Generation and Lithospheric Deformation at Mid-Ocean Ridges, Geophys. Monogr.* Washington, DC: Am. Geophys. Union. In press
Forsyth, D. W., Ehrenbard, R. L., Chapin, S. 1987. Anomalous upper mantle beneath the Australian-Antarctic discordance. *Earth Planet. Sci. Lett.* 84: 471–78
Fox, P. J., Schreiber, E., Peterson, J. J. 1973. The geology of the oceanic crust: Compressional wave velocities of oceanic rocks. *J. Geophys. Res.* 78: 5155–79
Francheteau, J., Ballard, R. D. 1983. The East Pacific Rise near 21°N, 13°N and 20°S: Inferences for along-strike variability of axial processes of the mid-ocean ridge. *Earth Planet. Sci. Lett.* 64: 93–116
Francis, T. J. G. 1969. Generation of seismic anisotropy along the mid-ocean ridges. *Nature* 221: 162–65
Garmany, J. 1989. Accumulations of melt at the base of young oceanic crust. *Nature* 340: 628–32
Girardin, N. 1980. Travel time residuals of PP waves reflected under oceanic and continental platform regions. *Phys. Earth. Planet. Inter.* 23: 199–206
Girardin, N., Jacoby, W. R. 1976. Rayleigh wave dispersion along Reykjanes Ridge. *Tectonophysics* 55: 155–71
Grand, S. P. 1987. Tomographic inversion for shear velocity beneath the North American plate. *J. Geophys. Res.* 92: 14,065–90
Hager, B. H., O'Connell, R. J. 1979. Kinematic models of large-scale flow in the Earth's mantle. *J. Geophys. Res.* 84: 1031–48
Hale, L. D., Morton, C. J., Sleep, N. H. 1982. Reinterpretation of seismic reflection data over the East Pacific Rise. *J. Geophys. Res.* 87: 7707–17
Harding, A. J., Orcutt, J. A., Kappus, M. E., Vera, E. E., Mutter, J. C., et al. 1989. Structure of young oceanic crust at 13°N on the East Pacific Rise from expanding spread profiles. *J. Geophys. Res.* 94: 12,163–96
Haymon, R. M., Fornari, D. J., Edwards, M. H., Carbotte, S., Wright, D., Mac-

donald, K. C. 1991. Hydrothermal vent distribution along the East Pacific Rise crest (9°09′–54′N) and its relationship to magmatic and tectonic processes on fast-spreading mid-ocean ridges. *Earth Planet. Sci. Lett.* 104: 513–34

Herron, T. J. 1982. Lava flow layer—East Pacific Rise. *Geophys. Res. Lett.* 9: 17–20

Herron, T. J., Ludwig, W. J., Stoffa, P. L., Kan, T. K., Buhl, P. 1978. Structure of the East Pacific Rise crest from multichannel seismic reflection data. *J. Geophys. Res.* 83: 798–804

Hess, H. H. 1964. Seismic anisotropy of the uppermost mantle under oceans. *Nature* 203: 629–31

Houtz, R., Ewing, J. 1976. Upper crustal structure as a function of plate age. *J. Geophys. Res.* 81: 2490–98

Huang, P. Y., Solomon, S. C. 1988. Centroid depths of mid-ocean ridge earthquakes: Dependence on spreading rate. *J. Geophys. Res.* 93: 13,445–77

Huang, P. Y., Solomon, S. C., Bergman, E. A., Nabelek, J. L. 1986. Focal depths and mechanisms of Mid-Atlantic Ridge earthquakes from body waveform inversion. *J. Geophys. Res.* 91: 579–98

Kent, G. M., Harding, A. J., Orcutt, J. A. 1990. Evidence for a smaller magma chamber beneath the East Pacific Rise at 9°30′N. *Nature* 344: 650–53

Kidd, R. G. W. 1977. A model for the process of formation of the upper oceanic crust. *Geophys. J. R. Astron. Soc.* 50: 149–83

Klein, E. M., Langmuir, C. H. 1989. Local versus global variations in ocean ridge basalt composition: A reply. *J. Geophys. Res.* 94: 4241–52

Kong, L. S. L., Solomon, S. C., Purdy, G. M. 1992. Microearthquake characteristics of a mid-ocean ridge along-axis high. *J. Geophys. Res.* In press

Kuo, B.-Y., Forsyth, D. W. 1988. Gravity anomalies of the ridge-transform system in the South Atlantic between 31 and 34.5°S: Upwelling centers and variations in crustal thickness. *Mar. Geophys. Res.* 10: 205–32

Kuo, B.-Y., Forsyth, D. W., Wysession, M. 1987. Lateral heterogeneity and azimuthal anisotropy in the North Atlantic determined from SS-S differential travel times. *J. Geophys. Res.* 92: 6421–36

Langmuir, C. H., Bender, J. F., Batiza, R. 1986. Petrological and tectonic segmentation of the East Pacific Rise, 5°30′–14°30′N. *Nature* 322: 422–29

Lees, A. R., Knopoff, L., Kausel, E. G. 1974. Variations of upper mantle structure under the Pacific Ocean. *Science* 186: 141–43

Lin, J., Bergman, E. A. 1990. Rift grabens, seismicity, and volcanic segmentation of the Mid-Atlantic Ridge: Kane to Atlantic fracture zones. *Eos, Trans. Am. Geophys. Union* 71: 1572 (Abstr.)

Lin, J., Purdy, G. M., Schouten, H., Sempere, J.-C., Zervas, C. 1990. Evidence from gravity data for focused magmatic accretion along the Mid-Atlantic Ridge. *Nature* 344: 627–32

Macdonald, K. C., Fox, P. J., Perram, L. J., Eisen, M. F., Haymon, R. M., et al. 1988. A new view of the mid-ocean ridge from the behaviour of ridge-axis discontinuities. *Nature* 335: 217–25

Macdonald, K. C., Luyendyk, B. P. 1977. Deep-tow studies of the structure of the Mid-Atlantic Ridge crest near lat 37°N. *Geol. Soc. Am. Bull.* 88: 621–36

McClain, J. S., Orcutt, J. A., Burnett, M. 1985. The East Pacific Rise in cross section: A seismic model. *J. Geophys. Res.* 90: 8627–39

McKenzie, D. 1979. Finite deformation during fluid flow. *Geophys. J. R. Astron. Soc.* 58: 689–715

McKenzie, D. 1984. The generation and compaction of partially molten rock. *J. Petrol.* 25: 713–65

Michael, P. J., Bonatti, E. 1985. Peridotite composition from the North Atlantic: Regional and tectonic variations and implications for partial melting. *Earth Planet. Sci. Lett.* 73: 91–104

Mitchell, B. J., Yu, G.-K. 1980. Surface wave dispersion, regionalized velocity models, and anisotropy of the Pacific crust and upper mantle. *Geophys. J. R. Astron. Soc.* 63: 497–514

Montagner, J. P., Jobert, N. 1983. Variation with age of the deep structure of the Pacific Ocean inferred from long-period Rayleigh wave dispersion. *Geophys. Res. Lett.* 27: 206–22

Montagner, J.-P., Tanimoto, T. 1990. Global anisotropy in the upper mantle inferred from the regionalization of phase velocities. *J. Geophys. Res.* 95: 4797–819

Morris, E., Detrick, R. S. 1991. Three-dimensional analysis of gravity anomalies in the MARK area, Mid-Atlantic Ridge 23°N. *J. Geophys. Res.* 96: 4355–66

Murase, T., McBirney, A. R. 1973. Properties of some common igneous rocks and their melts at high temperatures. *Geol. Soc. Am. Bull.* 84: 3563–92

Mutter, J. C., Barth, G. A., Buhl, P., Detrick, R. S., Orcutt, J., Harding, A. 1988. Magma distribution across ridge-axis discontinuities on the East Pacific Rise from multichannel seismic images. *Nature* 336: 156–58

Nishimura, C. E., Forsyth, D. W. 1985.

Anomalous Love-wave phase velocities in the Pacific: sequential pure-path and-spherical harmonic inversion. *Geophys. J. R. Astron. Soc.* 81: 389–407

Nishimura, C. E., Forsyth, D. W. 1988. Rayleigh wave phase velocities in the Pacific with implications for azimuthal anisotropy and lateral heterogeneities. *Geophys. J. R. Astron Soc.* 94: 479–501

Nishimura, C. E., Forsyth, D. W. 1989. The anisotropic structure of the upper mantle in the Pacific. *Geophys. J. R. Astron. Soc.* 96: 203–29

ODP (Ocean Drilling Program) Leg 106 Scientific Party 1986. Drilling the Snake Pit hydrothermal sulfide deposit on the Mid-Atlantic Ridge, lat 23°22′N. *Geology* 14: 1004–7

Pallister, J. S., Hopson, C. A. 1981. Samail ophiolite plutonic suite: Field relations, phase variation, cryptic variation and layering, and a model of a spreading ridge magma chamber. *J. Geophys. Res.* 86: 2593–644

Parsons, B., Sclater, J. G. 1977. An analysis of the variation of ocean floor bathymetry and heat flow with age. *J. Geophys. Res.* 82: 803–27

Phipps Morgan, J. 1987. Melt migration beneath mid-ocean spreading centers. *Geophys. Res. Lett.* 14: 1238–41

Phipps Morgan, J., Forsyth, D. W. 1988. Three-dimensional flow and temperature perturbations due to a transform offset: effects on oceanic crustal and upper mantle structure. *J. Geophys. Res.* 93: 2955–66

Purdy, G. M. 1982. The variability in seismic structure of layer 2 near the East Pacific Rise at 12°N. *J. Geophys. Res.* 87: 8403–16

Purdy, G. M., Detrick, R. S. 1986. Crustal structure of the Mid-Atlantic Ridge at 23°N from seismic refraction studies. *J. Geophys. Res.* 91: 3739–62

Raitt, R. W. 1963. The crustal rocks. In *The Sea*, Vol. 3, ed. M. N. Hill, pp. 85–102. New York: Wiley-Interscience

Raitt, R. W., Shor, G. G., Francis, T. J. G., Morris, G. B. 1969. Anisotropy of the Pacific upper mantle. *J. Geophys. Res.* 74: 3095–109

Reid, I., Jackson, H. R. 1981. Oceanic spreading rate and crustal thickness. *Mar. Geophys. Res.* 5: 165–72

Ribe, N. M. 1989. Seismic anisotropy and mantle flow. *J. Geophys. Res.* 94: 4213–23

Romanowicz, B. 1991. Seismic tomography of the Earth's mantle. *Annu. Rev. Earth Planet. Sci.* 19: 77–99

Rona, P. A., Klinkhammer, G., Nelson, T. A., Trefry, J. H., Elderfield, H. 1986. Black smokers, massive sulfides and vent biota at the Mid-Atlantic Ridge. *Nature* 321: 33–37

Schouten, H., Klitgord, K. D., Whitehead, J. A. 1985. Segmentation of mid-ocean ridges. *Nature* 317: 225–29

Scott, D. R., Stevenson, D. J. 1989. A self-consistent model of melting, magma migration and buoyancy-driven circulation beneath mid-ocean ridges. *J. Geophys. Res.* 94: 2973–88

Sempere, J.-C., Purdy, G. M., Schouten, H. 1990. Segmentation of the Mid-Atlantic Ridge between 24°N and 30°40′N. *Nature* 344: 427–31

Shearer, P., Orcutt, J. 1985. Anisotropy in the oceanic lithosphere—theory and observations from the Ngendei seismic refraction experiment in the south-west Pacific. *Geophys. J. R. Astron. Soc.* 80: 493–526

Sheehan, A. F., Solomon, S. C. 1991. Joint inversion of shear wave travel time residuals and geoid and depth anomalies for long-wavelength variations in upper mantle temperature and composition along the Mid-Atlantic Ridge. *J. Geophys. Res.* 96: 19,981–20,009

Shimamura, H. 1984. Anisotropy in the oceanic lithosphere of the northwestern Pacific basin. *Geophys. J. R. Astron. Soc.* 76: 253–60

Sleep, N. H. 1975. Formation of oceanic crust: Some thermal constraints. *J. Geophys. Res.* 80: 4037–42

Solomon, S. C., Huang, P. Y., Meinke, L. 1988. The seismic moment budget of slowly spreading ridges. *Nature* 334: 58–61

Spudich, P., Orcutt, J. 1980. A new look at the seismic velocity structure of the oceanic crust. *Rev. Geophys.* 18: 627–45

Toomey, D. R., Purdy, G. M., Solomon, S. C., Wilcock, W. S. D. 1990. The three-dimensional seismic velocity structure of the East Pacific Rise near latitude 9°30′N. *Nature* 347: 639–45

Toomey, D. R., Solomon, S. C., Purdy, G. M. 1988. Microearthquakes beneath the median valley of the Mid-Atlantic ridge near 23°N: Tomography and tectonics. *J. Geophys. Res.* 93: 9093–112

Toomey, D. R., Solomon, S. C., Purdy, G. M., Murray, M. H. 1985. Microearthquakes beneath the median valley of the Mid-Atlantic Ridge near 23°N: Hypocenters and focal mechanisms. *J. Geophys. Res.* 90: 5443–58

Vera, E. E., Mutter, J. C., Buhl, P., Orcutt, J. A., Harding, A. J., et al. 1990. The structure of 0- to 0.2-m.y.-old oceanic crust at 9°N on the East Pacific Rise from expanded spread profiles. *J. Geophys. Res.* 95: 15,529–56

Whitehead, J. A. Jr., Dick, H. J. B., Schouten, H. 1984. A mechanism for magmatic accretion under spreading centres. *Nature* 312: 146–48

Wilcock, W. S. D., Solomon, S. C., Purdy, G. M., Toomey, D. R., Dougherty, M. E. 1991. Seismic attenuation structure of the crust on the axis of the East Pacific Rise at 9°30′N. In *Spring Meeting 1991, Eos, Trans. Am. Geophys. Union* 72, suppl.: 263 (Abstr.)

Woodhouse, J. H., Dziewonski, A. M. 1984. Mapping the upper mantle: Three dimensional modeling of Earth structure by inversion of seismic waveforms. *J. Geophys. Res.* 89: 5953–86

Woodward, R. L., Masters, G. 1991. Global upper mantle structure from long-period differential travel times. *J. Geophys. Res.* 96: 6351–78

Yoshii, T. 1975. Regionality of group velocities of Rayleigh waves in the Pacific and the thickening of the plate. *Earth Planet. Sci. Lett.* 25: 305–12

Zhang, Y.-S., Tanimoto, T. 1989. Three-dimensional modelling of upper mantle structure under the Pacific Ocean and surrounding area. *Geophys. J. Int.* 98: 255–69

Zhang, Y.-S., Tanimoto, T. 1991. Global Love wave phase velocity variation and its significance to plate tectonics. *Phys. Earth Planet. Inter.* 66: 160–202

Annual Review of Earth and Planetary Sciences
Volume 20, 1992

CONTENTS